Supporting Information

Diverse Coordination Modes of Bidentate COC and Tridentate CNC Ligands Comprising 1,2,3-Triazol-5-ylidenes

Lewis C. Tolley,[a] Ian Strydom,[b] Wynand J. Louw,[b] Manuel A. Fernandes,[a]
Daniela I. Bezuidenhout,[a*] and Gregorio Guisado-Barrios,[c*]

[a] Molecular Sciences Institute, School of Chemistry, University of the Witwatersrand, Johannesburg 2050, South Africa

[b] Department of Chemistry, University of Pretoria, Private Bag X20, Hatfield 0028, Pretoria, South Africa

[c] Institute of Advance Materials (INAM), Centro de Innovación en Química Avanzada Universitat Jaume I, Avenida Vicente Sos Baynat s/n, 12071 Castellon, Spain

Email: *daniela.bezuidenhout@wits.ac.za, guisado@uji.es*

Contents

S1. General Methods

a. Method

All synthetic manipulations, unless otherwise stated, were performed under a N_2 (g) or Ar (g) atmosphere using oven or flame dried glassware and standard Schlenk or vacuum line techniques. Air sensitive solids were stored and handled in an InertLab glove box. Preparations of NMR and crystallization samples that also require an inert atmosphere were performed in a glove box.

b. Materials

The following ligand and metal precursors were synthesized in this study according to known synthetic procedures: 1,3-bis-(2,6-diisopropylphenyl)triaz-1-ene],[1] sodium hypochlorite,[2] N-(tert-butyloxy)carbonyl dipropargylamine,[3] di-μ-chloro-bis(1,5-cyclooctadiene)dirhodium(I),[4] di-μ-chloro-tetracarbonyldirhodium(I),[5] and di-μ-chloro-bis(1,5-cyclooctadiene)diiridium(I),[6] All other reagents were obtained from commercial sources and were used without any further purification.

Unless otherwise stated, only anhydrous solvents were used for the experimental procedures. Anhydrous THF (tetrahydrofuran) and DEE (diethyl ether) were obtained after distillation over sodium wire Na(s) and benzophenone under a N_2 (g) atmosphere. Anhydrous toluene and hexane were obtained after distillation over sodium wire under a N_2 (g) atmosphere. Anhydrous DCM (dichloromethane) was obtained after distillation over calcium hydride (CaH_2) under a N_2 (g) atmosphere. Deuterated benzene was dried over sodium and distilled under an Ar (g) atmosphere. Deuterated acetonitrile, chloroform and dichloromethane were dried over calcium hydride under an Ar (g) atmosphere.

b. Characterization Techniques

Nuclear magnetic resonance (NMR) spectra were obtained using either a Bruker AVANCE-III-300 operating at 300.13 MHz for ^{1}H, 75.47 MHz for ^{13}C, 121.49 MHz for ^{31}P and 282.40 MHz for ^{19}F; or AVANCE-III-400 operating at 400.21 MHz for ^{1}H, 100.64 MHz for ^{13}C, 162.01 MHz for ^{31}P and 376.57 MHz for ^{19}F; or AVANCE-III-500 operating at 500.13 MHz for ^{1}H, 125.31 MHz for ^{13}C, 202.46 MHz for ^{31}P and 470.59 MHz for ^{19}F. ^{1}H Chemical shifts are reported as δ (ppm) values downfield from Me_4Si and chemical shifts were referenced to residual non-deuterated solvent peaks ($CDCl_3$: 7.260 ppm, C_6D_6: 7.160 ppm; CD_2Cl_2: 5.32 ppm; and CD_3CN: 1.940 ppm). ^{13}C chemical shifts are also reported as δ (ppm) values

downfield from Me_4Si and chemical shifts were referenced to residual non-deuterated solvents peaks ($CDCl_3$: 77.160 ppm, C_6D_6: 128.060 ppm; CD_2Cl_2: 54.00 ppm; and CD_3CN: 118.260 ppm. Proton coupling constants (*J*) are given in Hz. The spectral coupling patterns are designated as follows: s - singlet; d - doublet; t - triplet; q- quartet; quint – quintet; sept - septet; m - multiplet; dd- doublet of doublets; dt – doublet of triplets; td – triplet of doublets; br - broad signal. Quaternary carbons are designated as $\mathbf{C}_q$.

Chemical shift assignment in the ^1H NMR spectra is based on first-order analysis experiments. The ^{13}C shifts were obtained from proton-decoupled ^{13}C NMR spectra. Where necessary, the multiplicities of the ^{13}C signals were deduced from proton-decoupled DEPT-135 spectra. The resonances of the proton-bearing carbon atoms were correlated with specific proton resonances using 2D (^{13}C-^1H) heteronuclear single-quantum coherence (HSQC) experiments. Standard Bruker pulse programs (298 K) were used in the experiments, while low temperature (243 K) NMR experiments were run for all of the fluxional 1,5-cyclooctadiene metal complexes.

Solution IR spectra (ν(CO)) were recorded on a Bruker ALPHA FT–IR spectrophotometer in CH_2Cl_2 as solvent. The range of absorption measured was from 4000-400 cm^{-1}.

Electrospray mass spectra (ESI-MS) were recorded on a Bruker QTOF Mass spectrometer with positive electron spray as the ionization techniques; nitrogen was employed as drying and nebulizing gas at a flow of 4 L/min. The m/z values were measured in the range of 100-1500 with acetonitrile as solvent. Accurate mass measurements were performed by use of a Q-TOF premier mass spectrometer with electrospray source (Waters, Manchester, UK) operating at a resolution of ca. 16 000 (fwhm).

S2. Synthesis and characterization of ligand precursors

Synthesis of $[H_2(COC)](PF_6)_2$

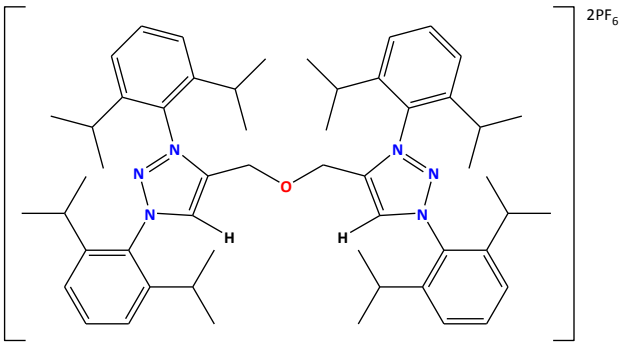

A round-bottom flask was loaded with dry 1,3-bis-(2,6-diisopropylphenyl)triaz-1-ene (14.62 g, 0.04 mol), KPF_6 (7.36 g, 0.04 mol), and degassed CH_2Cl_2 (*ca.* 500 mL). Whilst stirring, dipropargyl ether (0.69 mL, 6.69 mmol) was added to the reaction vessel and cooled to -78°C. ^{t}BuOCl (4.55 mL, 0.04 mol) was added dropwise in the absence of light, and allowed to warm to room temperature (RT) overnight. The solvent was evaporated under reduced pressure, and the residue was washed with dichloromethane (DCM) to yield a pinkish-white solid. Excess KPF_6 was removed by performing multiple H_2O/DCM (50/50) liquid-liquid extractions. Combined organic fractions were then evaporated to dryness and the resulting solid washed with diethyl ether to yield $[H_2(\mathbf{COC})](PF_6)_2$ (6.46 g, 5.8 mmol, 87%), as a white solid after vacuum filtration. Crystallization from DCM yielded single crystals suitable for XRD analysis.

^{1}H NMR δ_H (CD_3CN, 500.13 MHz) 8.91 (s, 2H, C**H**$_{\mathbf{Trz}}$), 7.76 (td, 4H, *J*= 7.9 Hz, Ar**H**$_{Dipp}$), 7.54 (dd, 8H, *J*= 7.9 Hz, 7.85 Hz, Ar**H**$_{Dipp}$), 4.58 (s, 4H, O(C**H**$_2$)$_2$), 2.21 (sept, 4H, *J*= 6.9 Hz, C**H**(CH$_3$)$_2$), 2.10 (sept, 4H, *J*= 6.7 Hz, C**H**(CH$_3$)$_2$), 1.29 (d, 12H, *J*= 6.8 Hz, CH(C**H**$_3$)$_2$), 1.18 (dd, 24H, *J*= 6.9 Hz, 7.0 Hz, CH(C**H**$_3$)$_2$), 1.10 (d, 12H, J= 6.8 Hz, CH(C**H**$_3$)$_2$) **^{13}C NMR** δ_C (CD_3CN,125.31 MHz) δ146.54 (Ar**C**$_q$), 146.27 (Ar**C**$_q$), 143.43 (**C**$_{q\ Trz}$), 134.92 (**C**H$_{Trz}$), 134.82, (Ar**C**H) 134.58 (Ar**C**H), 131.19 (Ar**C**$_q$), 128.78 (Ar**C**$_q$), 126.47 (Ar**C**H), 126.13 (Ar**C**H), 62.17 (O(**C**H$_2$)$_2$), 3t0.17 (**C**H(CH$_3$)$_2$), 30.02 (**C**H(CH$_3$)$_2$), 25.60 (CH(**C**H$_3$)$_2$), 24.78 (CH(**C**H$_3$)$_2$), 23.88 (CH(**C**H$_3$)$_2$), 22.85 (CH(**C**H$_3$)$_2$) **^{19}F NMR** δ_F (CD_3CN, 470.59 MHz) -72.81 (d, *J* = 707.4 Hz, P**F**$_6$) **^{31}P NMR** δ_P (CD_3CN, 202.46 MHz) -144.58 (sept, *J* = 707.0 Hz, **P**F$_6$). **HRMS** (FIA-ESI): Calculated for $[C_{54}H_{74}N_6O]^{2+}$ $[M - 2PF_6]^{2+}$: 411.2962; found: 411.2946, $[C_{54}H_{74}N_6OPF_6]^+$ $[M - PF_6]^+$: 967.5565; found: 967.5456.

Synthesis of $[H_2(C^{Boc}NC)](PF_6)_2$

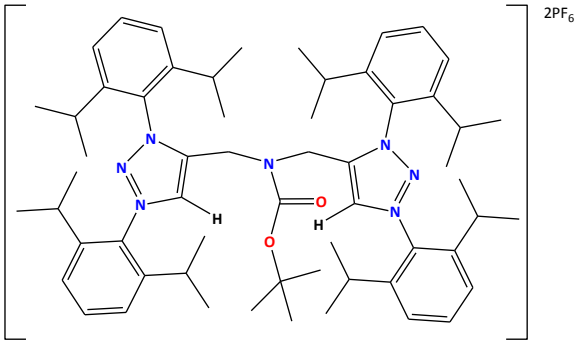

Compound $[H_2(\mathbf{C^{Boc}NC})](PF_6)_2$ was prepared by a similar procedure as employed for the synthesis of $[H_2(\mathbf{COC})](PF_6)_2$. A round bottom flask (RBF) was loaded with 1,3-bis-(2,6-diisopropylphenyl)triaz-1-ene (28.4 g, 0.08 mol), KPF_6 (17.2 g, 0.09 mol), N-(tert-butyloxy)carbonyl dipropargylamine (5.0 g, 0.03 mol) and degassed, anhydrous DCM (*ca.* 500 mL). After cooling the reaction mixture to -78°C, ^{t}BuOCl (8.8 mL, 0.08 mmol) was added dropwise in the absence of light and allowed to warm to RT overnight. The solvent was evaporated under reduced pressure, and the resulting solid was repeatedly washed with hexane, followed by diethyl ether (DEE), to yield $[H_2(\mathbf{C^{Boc}NC})](PF_6)_2$ (16.9 g, 0.014 mol, 54%) as a cream-coloured solid. Crystallization from DCM yielded single crystals suitable for XRD analysis.

^{1}H NMR δ_H (CD_3CN, 500.13 MHz) 8.97 (s, 1H, C**H**$_{Trz}$), 8.83 (S, 1H, C**H**$_{Trz}$), 7.77 (m, 3H, Ar**H**$_{Dipp}$), 7.54 (m, 9H, Ar**H**$_{Dipp}$), 4.60 (s, 2H, N(C**H**$_2$)$_2$), 3.71 (s, 2H, N(C**H**$_2$)$_2$), 2.25 (Sept, 6H, *J*= 6.6 Hz, C**H**(CH$_3$)$_2$), 2.12 (sept, 2H, *J*= 6.5 Hz, C**H**(CH$_3$)$_2$), 1.39 (s, 9H, C(C**H**$_3$)$_3$), 1.28 (dd, 18H, *J*= 7.9 Hz, 7.9 Hz, CH(C**H**$_3$)$_2$), 1.23 (d, 12H, *J*= 6.6 Hz, CH(C**H**$_3$)$_2$), 1.16 (d, 12H, *J*= 6.6 Hz, CH(C**H**$_3$)$_2$), 1.07 (dd, 6H, *J*= 6.5 Hz, 6.5 Hz, CH(C**H**$_3$)$_2$). **^{13}C NMR** δ_C (CD_3CN, 125.31 MHz) δ154.58 (BOC-**C**O), 146.64 (Ar**C**H), 146.30 (Ar**C**H), 146.18 (Ar**C**$_q$), 145.99, (Ar**C**$_q$) 145.18 (**C**$_{q\ Trz}$), 135.11 (Ar**C**H), 134.49 (**C**H $_{Trz}$), 133.67 (Ar**C**H), 131.17 (Ar**C**$_q$), 130.98 (Ar**C**$_q$), 128.99 (Ar**C**$_q$), 128.53 (Ar**C**$_q$), 126.63 (Ar**C**H), 126.10 (Ar**C**H), 85.25 (O**C**(CH$_3$)$_3$), 45.28 (N(**C**H$_2$)$_2$), 44.86 (N(**C**H$_2$)$_2$), 30.22 (**C**H(CH$_3$)$_2$), 29.96 (**C**H(CH$_3$)$_2$), 29.83 (**C**H(CH$_3$)$_2$), 29.81 (**C**H(CH$_3$)$_2$), 28.31 (CH(**C**H$_3$)$_2$), 26.45 (CH(**C**H$_3$)$_2$), 26.13 (CH(**C**H$_3$)$_2$), 25.09 (CH(**C**H$_3$)$_2$), 24.64 (CH(**C**H$_3$)$_2$), 24.02 (CH(**C**H$_3$)$_2$), 22.75 (CH(**C**H$_3$)$_2$), 22.47 (CH(**C**H$_3$)$_2$). **^{19}F NMR** δ_F (CD_3CN, 470.59 MHz) -72.85 (d, *J* = 705.8 Hz, P**F**$_6$). **^{31}P NMR** δ_P (CD_3CN, 202.46 MHz) -144.60 (d, *J* = 706.4 Hz, **P**F$_6$). **HRMS** (FIA-ESI): Calculated for $[C_{59}H_{83}N_7O_2]^{2+}$ [M – $2PF_6$]$^{2+}$: 460.8304; found: 460.8295, $[C_{59}H_{83}N_7O_2PF_6]^+$ [M – PF_6]$^+$: 1066.6250; found: 1066.6184 .

Synthesis of $[H_2(C^{H}NC)](PF_6)_2$

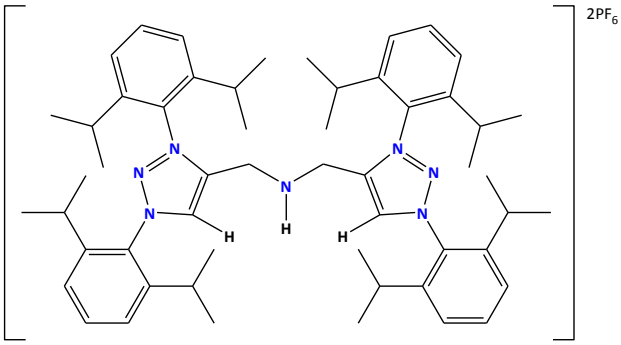

Compound $[H_2(\mathbf{C^{H}NC})](PF_6)_2$ was obtained by a simple deprotection strategy whereby compound $[H_2(\mathbf{C^{Boc}NC})](PF_6)_2$ (16.9 g, 0.014 mol) was treated with 3N methanolic HCl (60 mL, 0.181 mol) and was stirred for 2 days at 50°C. The solution was neutralized with saturated $NaHCO_3$ (aq), further basified with KOH (aq) until pH tested above 9 before frit filtration and solvent removal. Excess KPF_6 was removed by performing multiple H_2O/DCM (50/50) liquid-liquid extractions. The organic fractions were combined and then evaporated to dryness. The product was washed with hexane, DEE and DCM, consecutively, to yield $[H_2(\mathbf{C^{H}NC})](PF_6)_2$ (13.2 g, 0.012 mol, 85%) as a pure white solid. Crystallization from DCM yielded single crystals suitable for XRD analysis.

^{1}H NMR δ_H (CD_3CN, 500.13 MHz) 10.46 (s, 2H, C**H**$_{Trz}$), 7.71 (td, 4H, *J*= 7.8, Ar**H**$_{Dipp}$), 7.51 (dd, 8H, *J* = 7.8 Hz Ar**H**$_{Dipp}$), 4.44 (pent, 1H, N-**H**), 3.82 (d, 4H, *J*= 6.9 Hz, N(C**H**$_2$)$_2$), 2.23 (sept, 4H, *J*= 6.7 Hz, C**H**(CH$_3$)$_2$), 2.21 (Sept, 4H, *J*= 6.7 Hz, C**H**(CH$_3$)$_2$), 1.28 (d, 12H, *J*= 6.7 Hz, C**H**(CH$_3$)$_2$), 1.19 (d, 12H, *J* = 6.7 Hz, C(C**H**$_3$)$_3$), 1.15 (d, 12H, *J*= 6.8 Hz, CH(C**H**$_3$)$_2$), 1.08 (d, 12H, *J*= 6.8 Hz, CH(C**H**$_3$)$_2$). **^{13}C NMR** δ_C (CD_3CN,125.31 MHz) δ147.16 (Ar**C**$_q$), 146.51 (Ar**C**$_q$), 146.32 (**C**$_{q\ Trz}$), 136.26 (**C**H $_{Trz}$), 134.46 (Ar**C**H) 134.16 (Ar**C**H), 131.62 (Ar**C**$_q$), 129.02 (Ar**C**$_q$), 126.31 (Ar**C**H), 125.93 (Ar**C**H), 43.59 (N(**C**H$_2$)$_2$), 29.95 (**C**H(CH$_3$)$_2$), 29.88 (**C**H(CH$_3$)$_2$), 25.42 (CH(**C**H$_3$)$_2$), 24.56 (CH(**C**H$_3$)$_2$), 24.20 (CH(**C**H$_3$)$_2$), 23.04 (CH(**C**H$_3$)$_2$). **^{19}F NMR** δ_F (CD_3CN, 470.59 MHz) -72.81 (d, *J* = 706.4 Hz, P**F**$_6$). **^{31}P NMR** δ_P (CD_3CN, 202.46 MHz) -144.58 (d, *J* = 707.0 Hz, **P**F$_6$). **HRMS** (FIA-ESI): Calculated for $[C_{54}H_{75}N_7]^{2+}$ [M – 2PF$_6$]$^{2+}$: 410.8041 found: 410.8075, and also $[C_{54}H_{75}N_7PF_6]^{+}$ [M – PF$_6$]$^{+}$: 966.5725 found: 966.5674.

S3. NMR Spectra

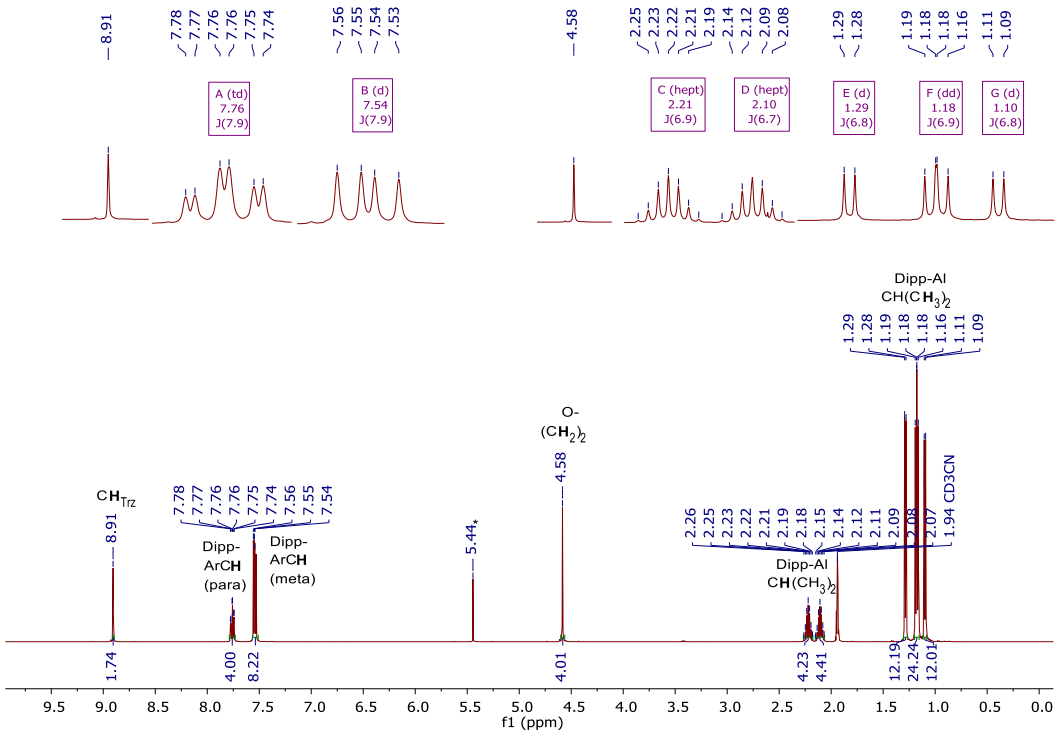

Figure S1: ^{1}H NMR spectrum of $[H_2(\mathbf{COC})](PF_6)_2$ in CD_3CN. [* annotates residual DCM ($C\mathbf{H}_2Cl_2$)]

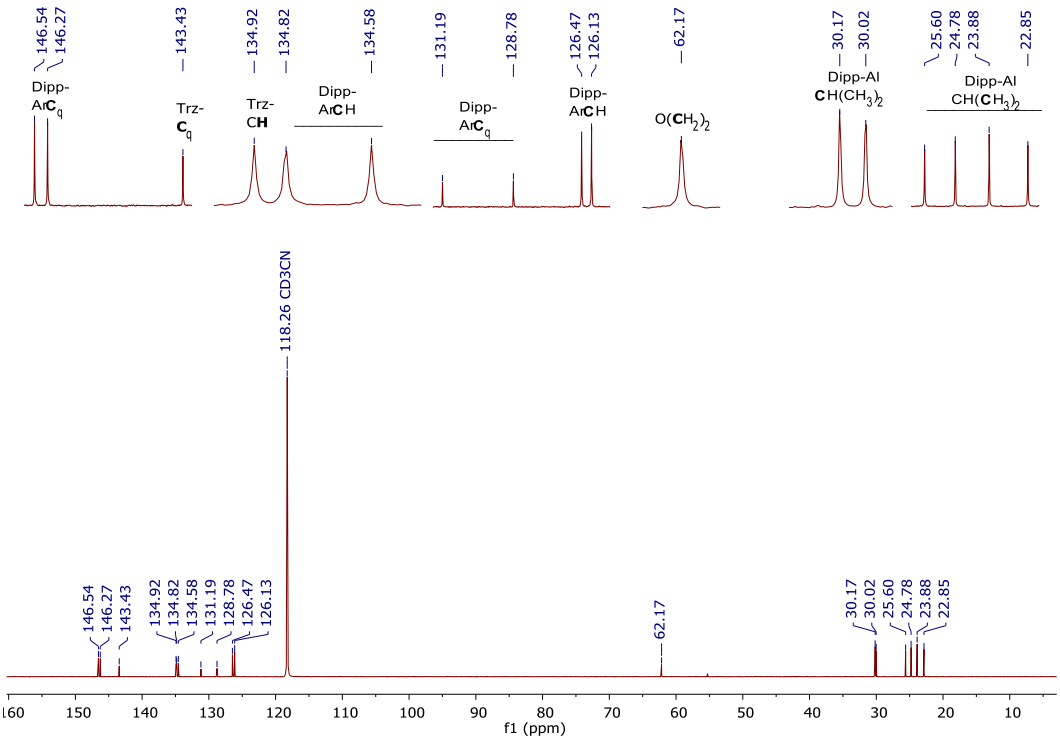

Figure S2: ^{13}C NMR spectrum of $[H_2(\mathbf{COC})](PF_6)_2$ in CD_3CN

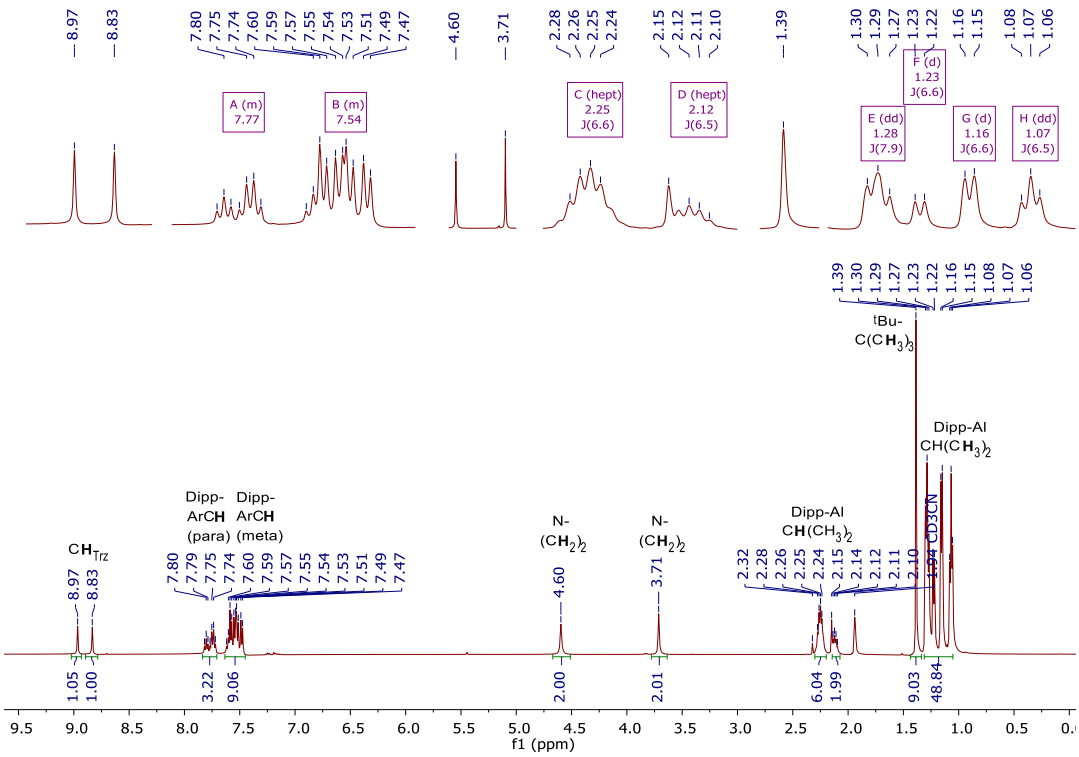

Figure S3: ^{1}H NMR spectrum of $[H_2(\mathbf{C^{Boc}NC})](PF_6)_2$ in CD_3CN

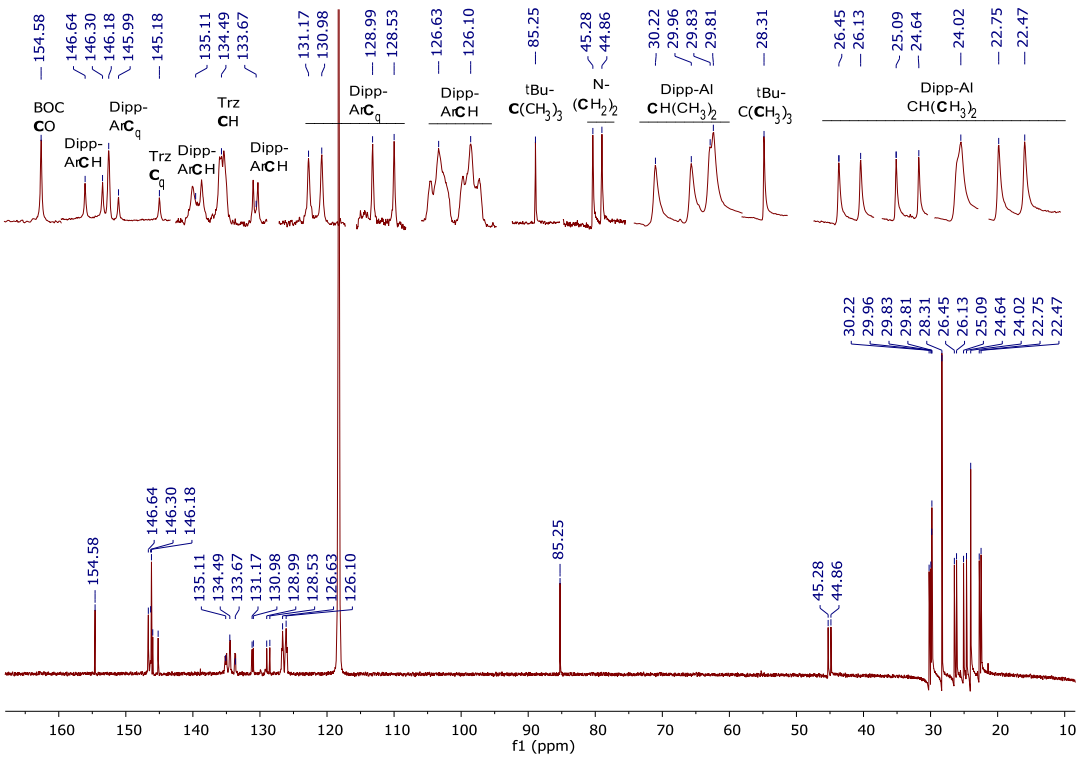

Figure S4: ^{13}C NMR spectrum of $[H_2(\mathbf{C^{Boc}NC})](PF_6)_2$ in CD_3CN

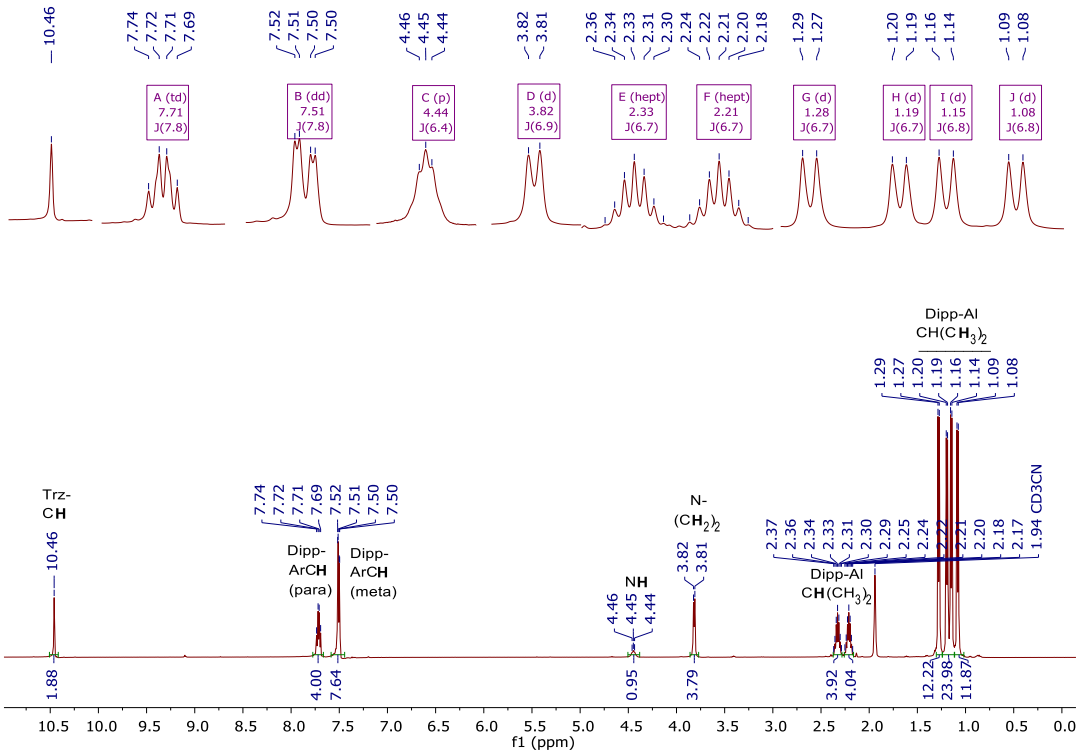

Figure S5: ^{1}H NMR spectrum of $[H_2(C^{H}NC)](PF_6)_2$ in CD_3CN

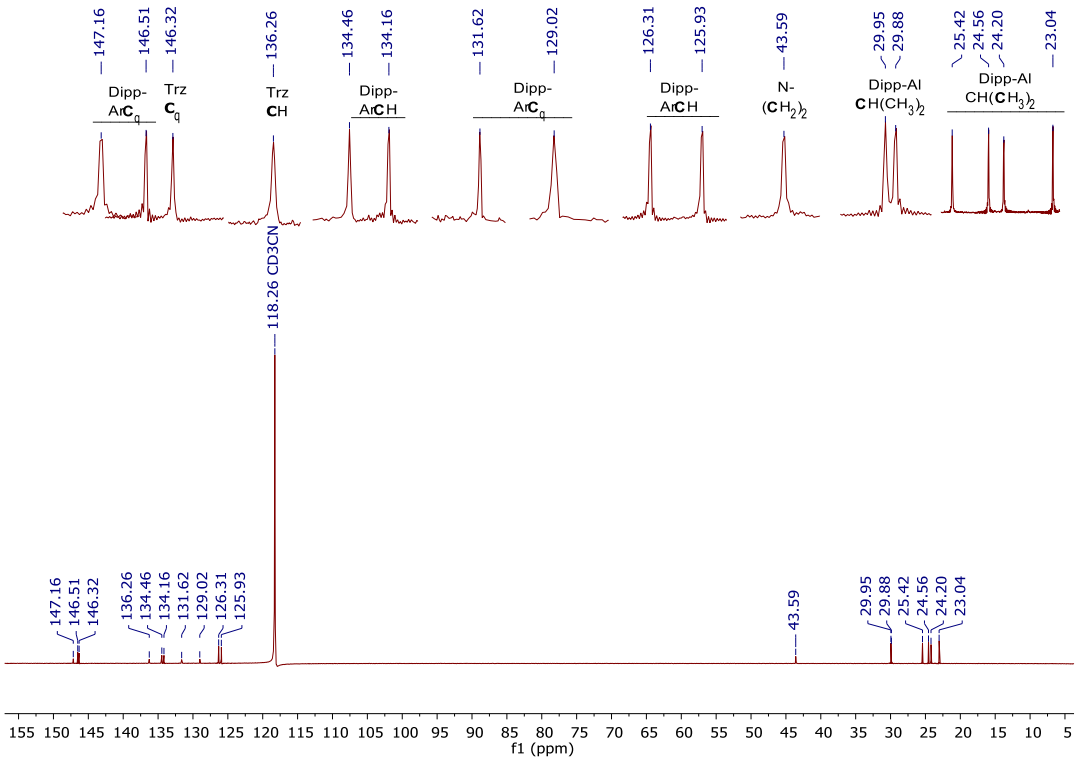

Figure S6: ^{13}C NMR spectrum of $[H_2(C^{H}NC)](PF_6)_2$ in CD_3CN

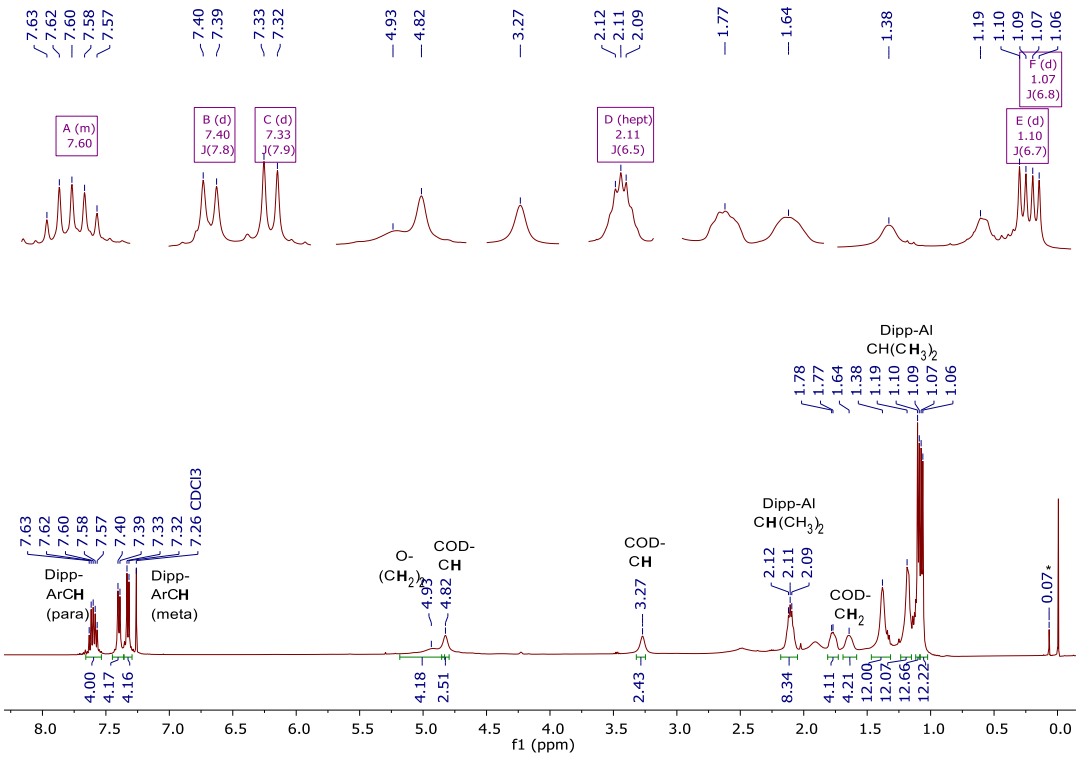

Figure S7: ^{1}H NMR spectrum of **1a** [Rh(cod)(**COC**)](PF$_6$) in CDCl$_3$ [* annotates grease]

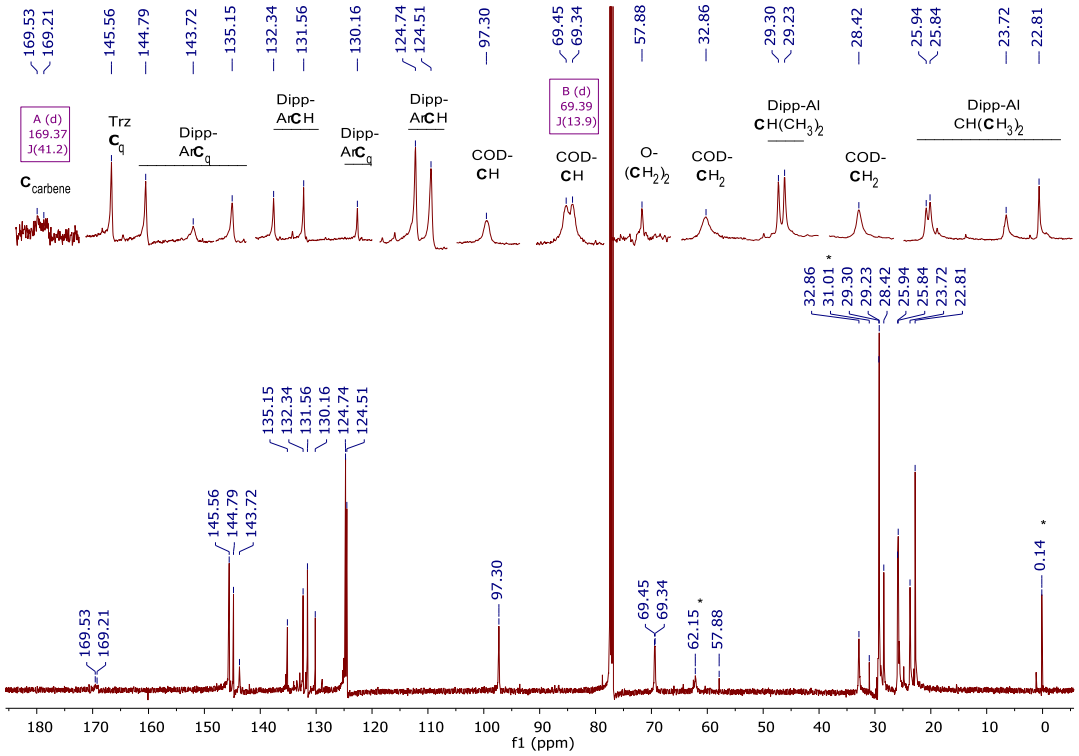

Figure S8: ^{13}C NMR spectrum of **1a** [Rh(cod)(**COC**)](PF$_6$) in CDCl$_3$ [* annotates grease]

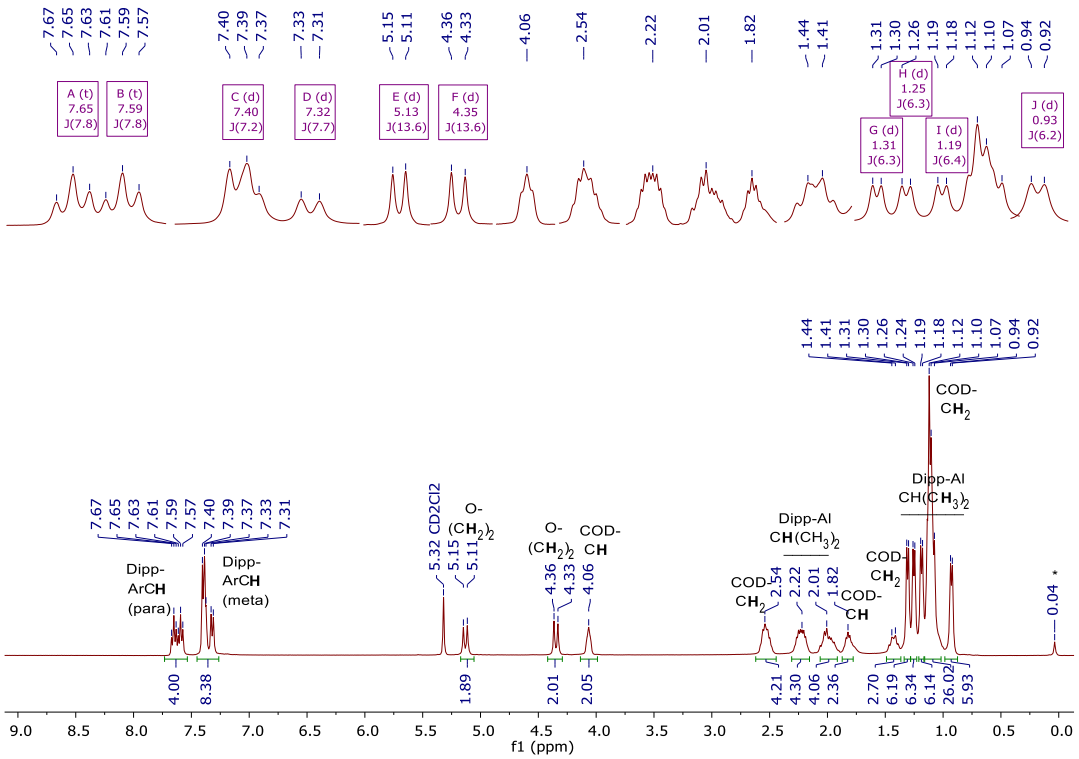

Figure S9: ^{1}H NMR spectrum (243 K) of **1b** [Ir(cod)(**COC**)](PF$_6$) in CD_2Cl_2 [* annotates grease]

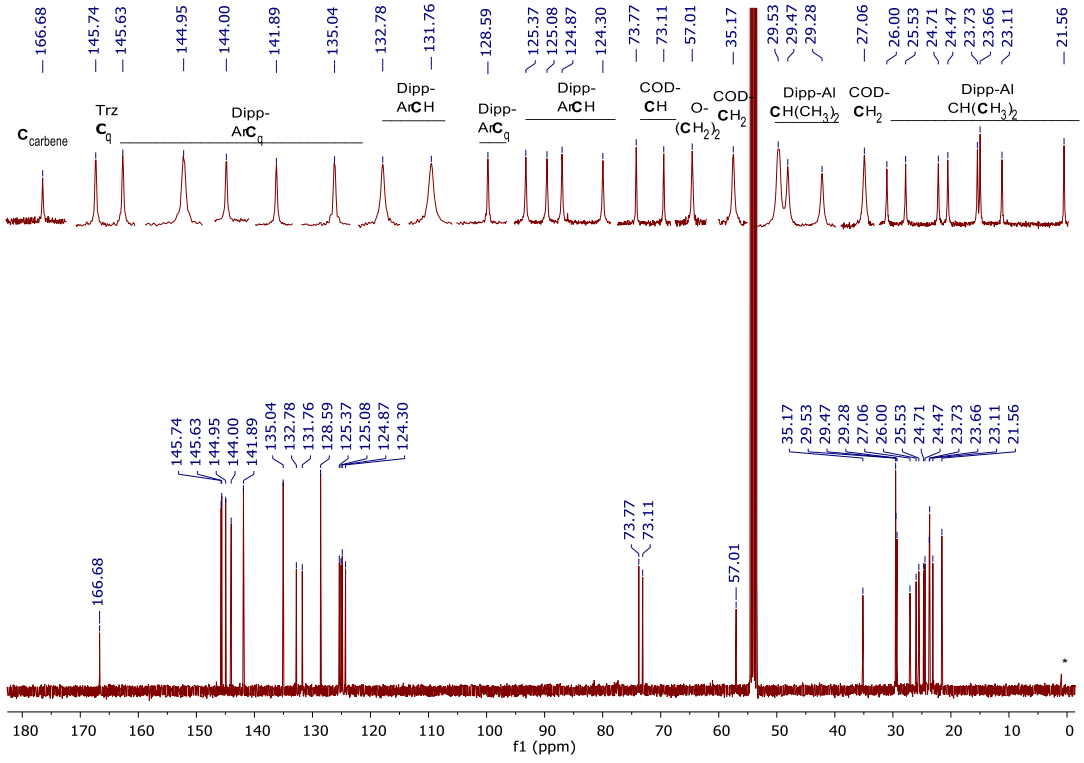

Figure S10: ^{13}C NMR spectrum (243 K) of **1b** [Ir(cod)(**COC**)](PF$_6$) in CD_2Cl_2 [* annotates grease]

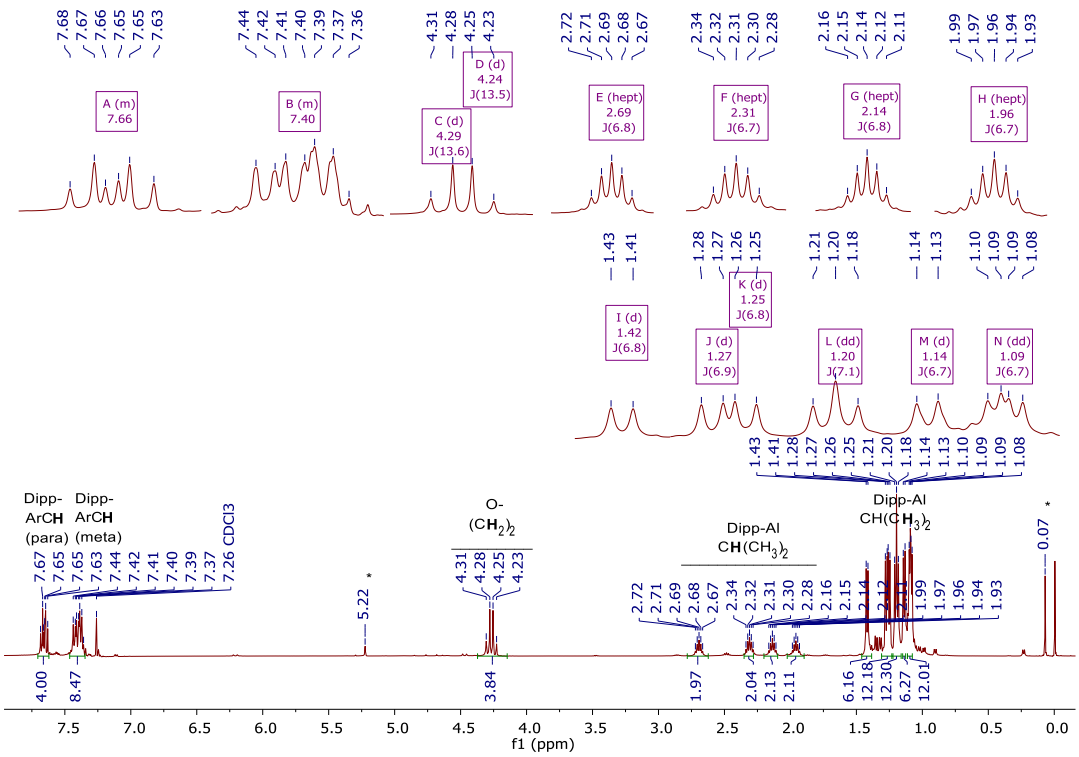

Figure S11: ^{1}H NMR spectrum of **2a** $[Rh(CO)_2(\mathbf{COC})](PF_6)$ in $CDCl_3$

[* annotates residual DCM ($C\mathbf{H}_2$) and grease]

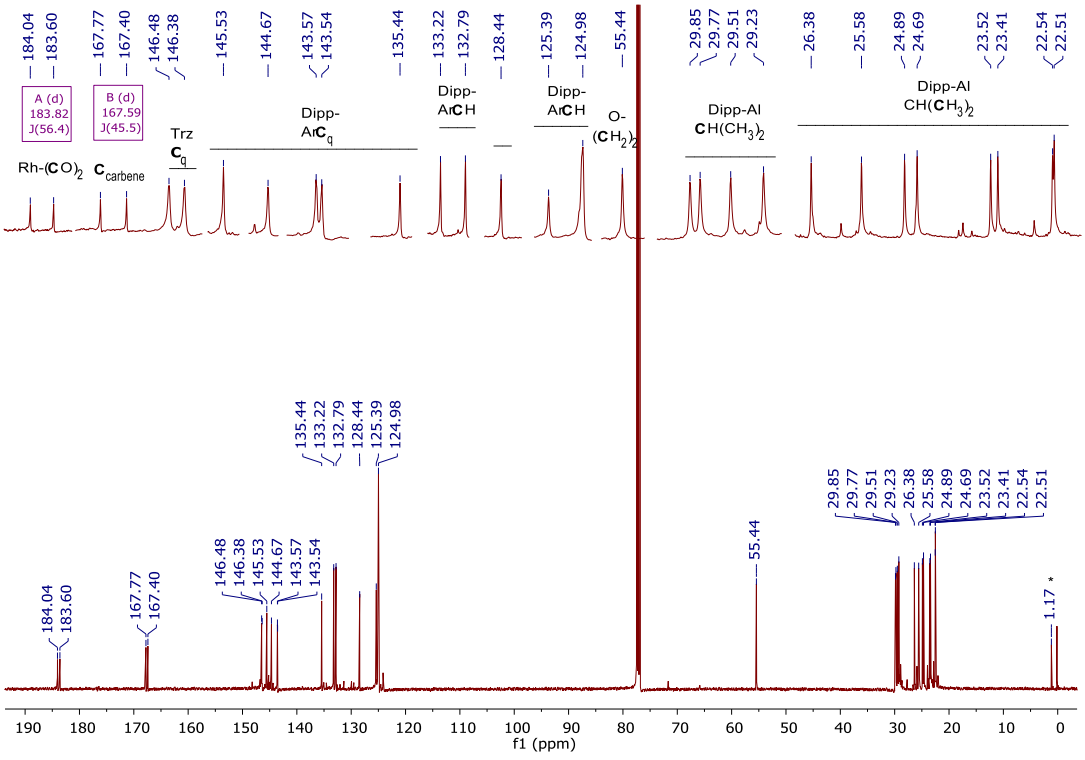

Figure S12: ^{13}C NMR spectrum of **2a** $[Rh(CO)_2(\mathbf{COC})](PF_6)$ in $CDCl_3$ [* annotates grease]

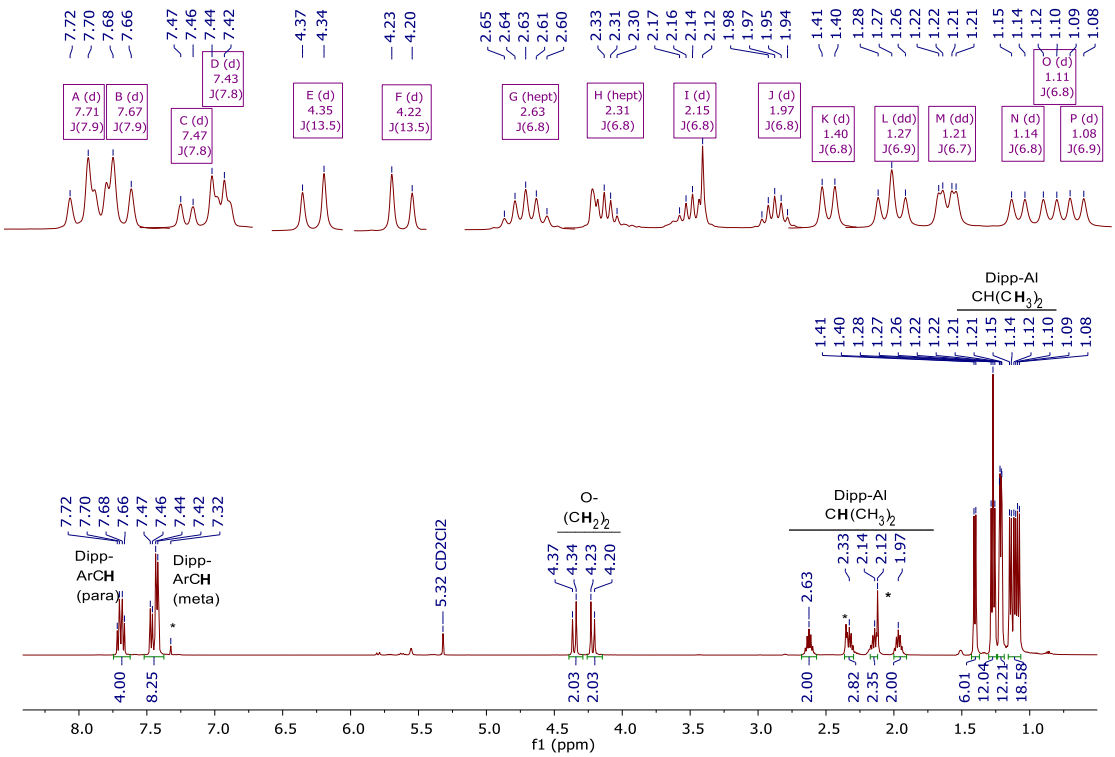

Figure S13: ^{1}H NMR spectrum of **2b** [Ir(CO)$_2$(**C**O**C**)](PF$_6$) in CD_2Cl_2

[* annotates residual chloroform (C**H**), toluene (C**H**$_3$), and acetone (C**H**$_3$)]

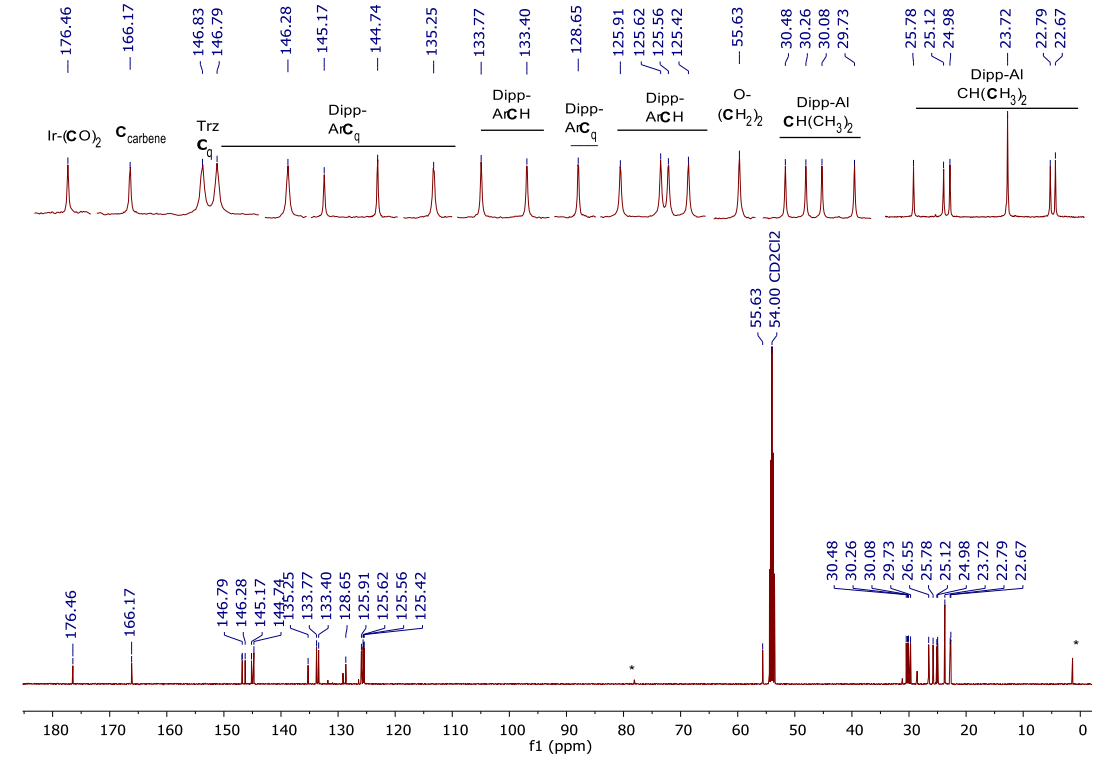

Figure S14: ^{13}C NMR spectrum of **2b** [Ir(CO)$_2$(**C**O**C**)](PF$_6$) in CD_2Cl_2

[* annotates residual chloroform (**C**H) and grease]

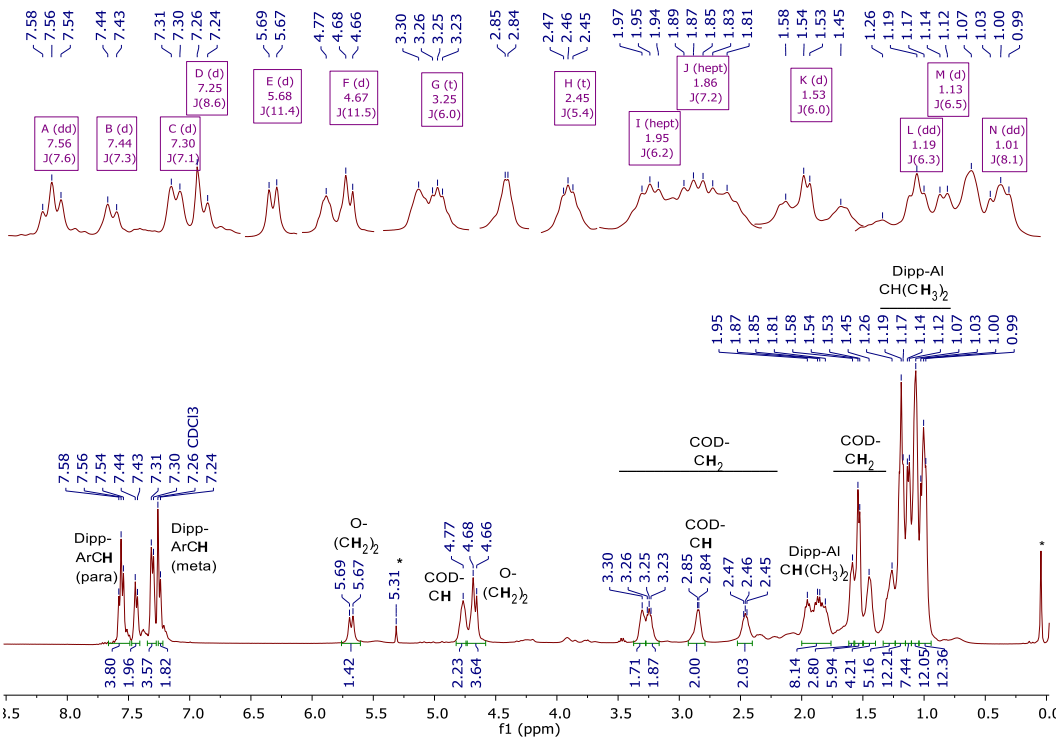

Figure S15: ^{1}H NMR spectrum (243 K) of **3a** [$Rh_2(cod)_2Cl_2$(μ-**COC**)] in $CDCl_3$

[* annotates residual DCM ($C\mathbf{H}_2Cl_2$) and grease]

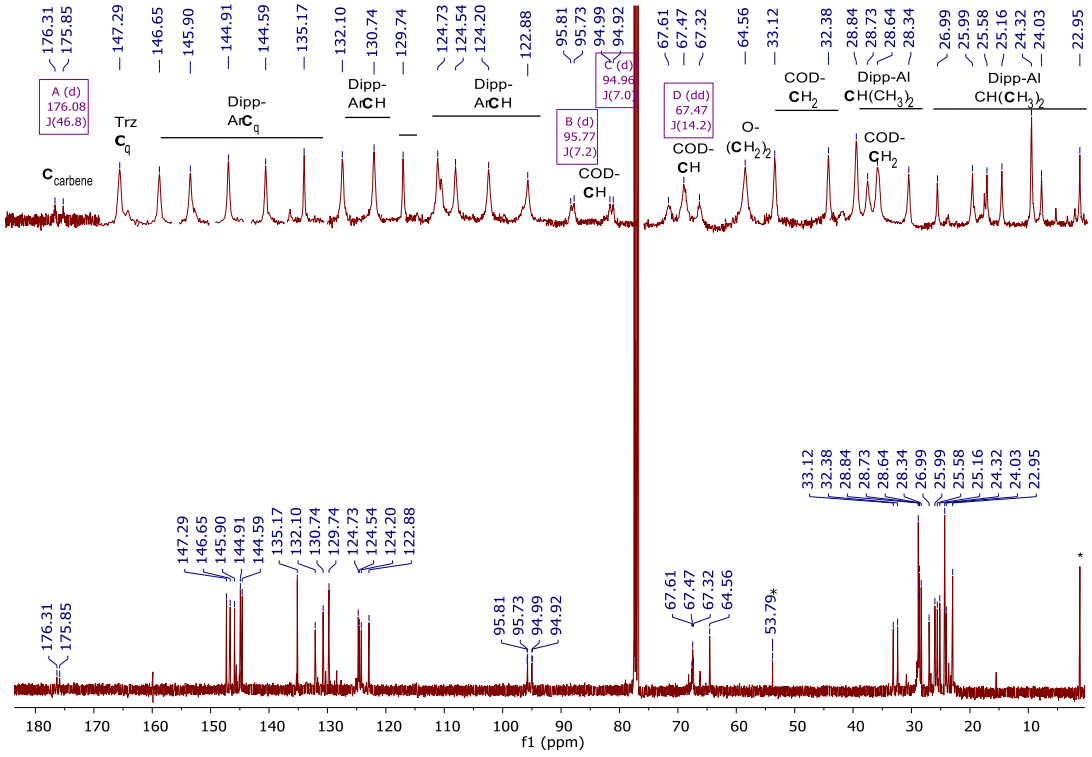

Figure S16: ^{13}C NMR spectrum (243 K) of **3a** [$Rh_2(cod)_2Cl_2$(μ-**COC**)] in $CDCl_3$

[* annotates residual DCM ($C\mathbf{H}_2Cl_2$) and grease]

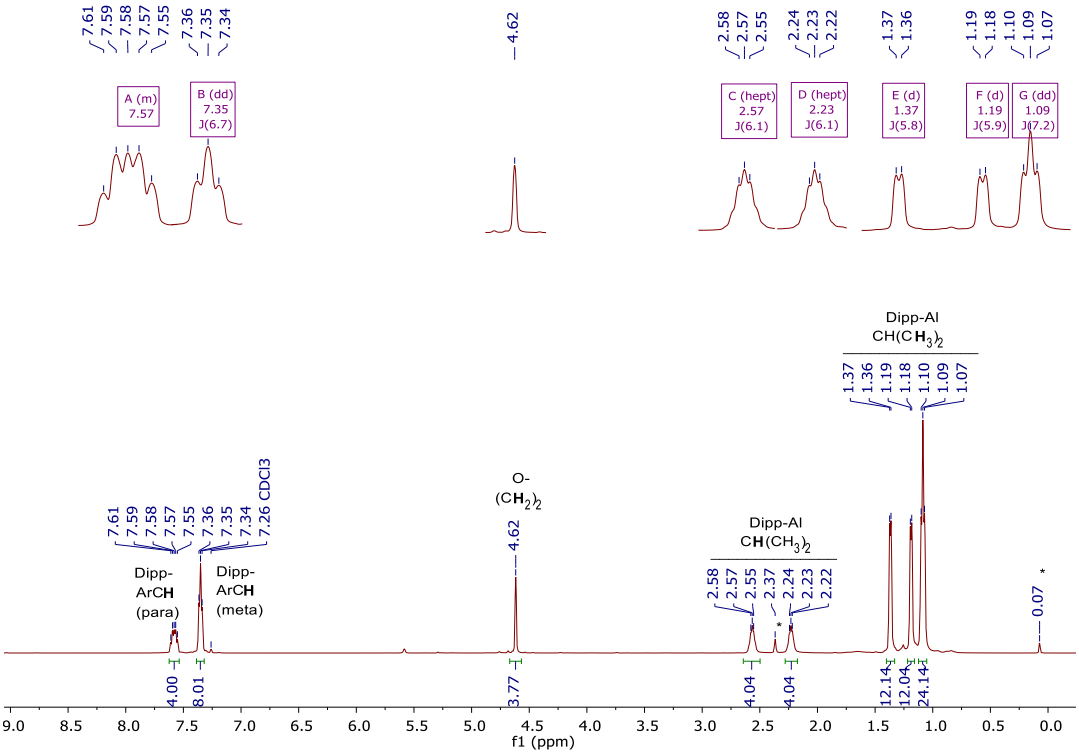

Figure S17: ^{1}H NMR spectrum of **4a** [$Rh_2(CO)_4Cl_2$(μ-**COC**)] in $CDCl_3$

[* annotates residual toluene (C**H**$_3$) and grease]

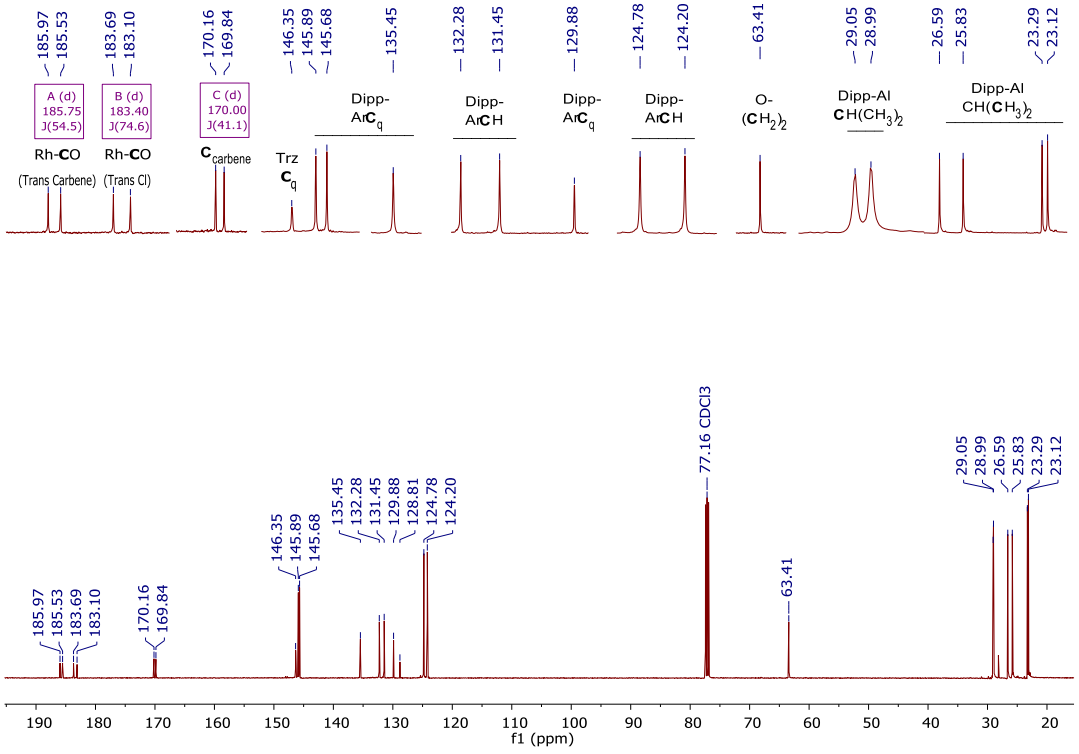

Figure S18: ^{13}C NMR spectrum of **4a** [$Rh_2(CO)_4Cl_2$(μ-**COC**)] in $CDCl_3$

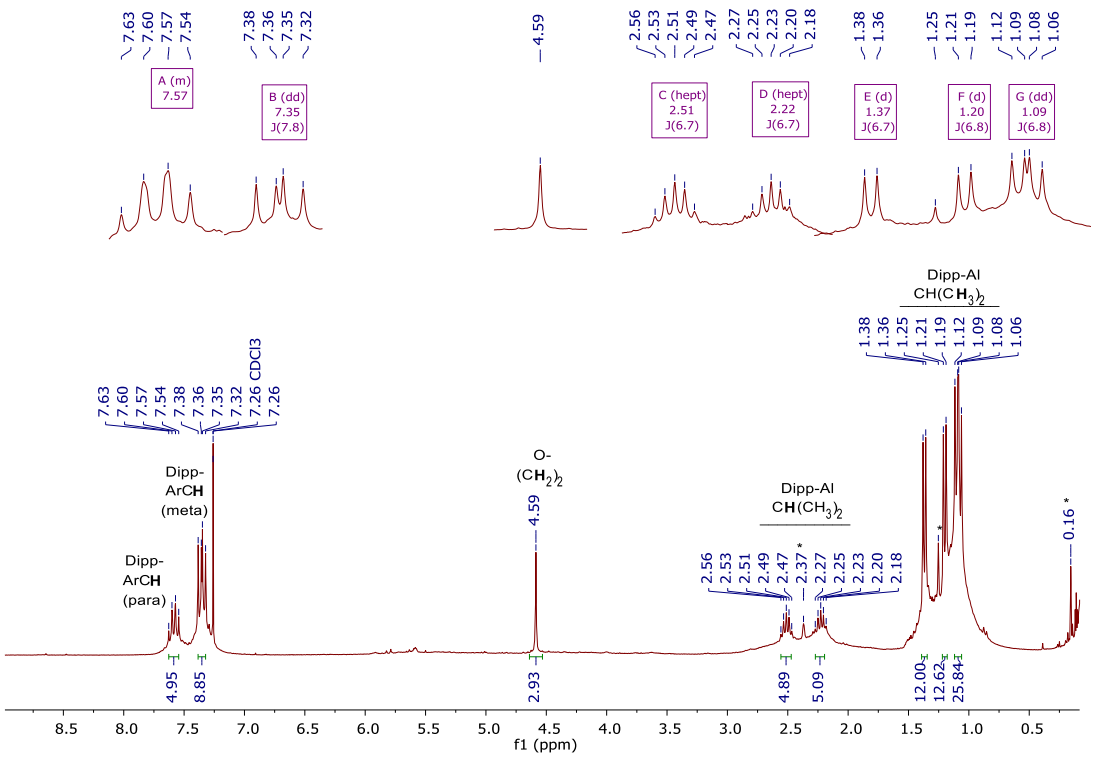

Figure S19: ^{1}H NMR spectrum of **4b** $[Ir_2(CO)_4Cl_2(\mu\text{-}\mathbf{COC})]$ in solvent $CDCl_3$ [* annotates residual toluene ($C\mathbf{H}_3$) and grease]

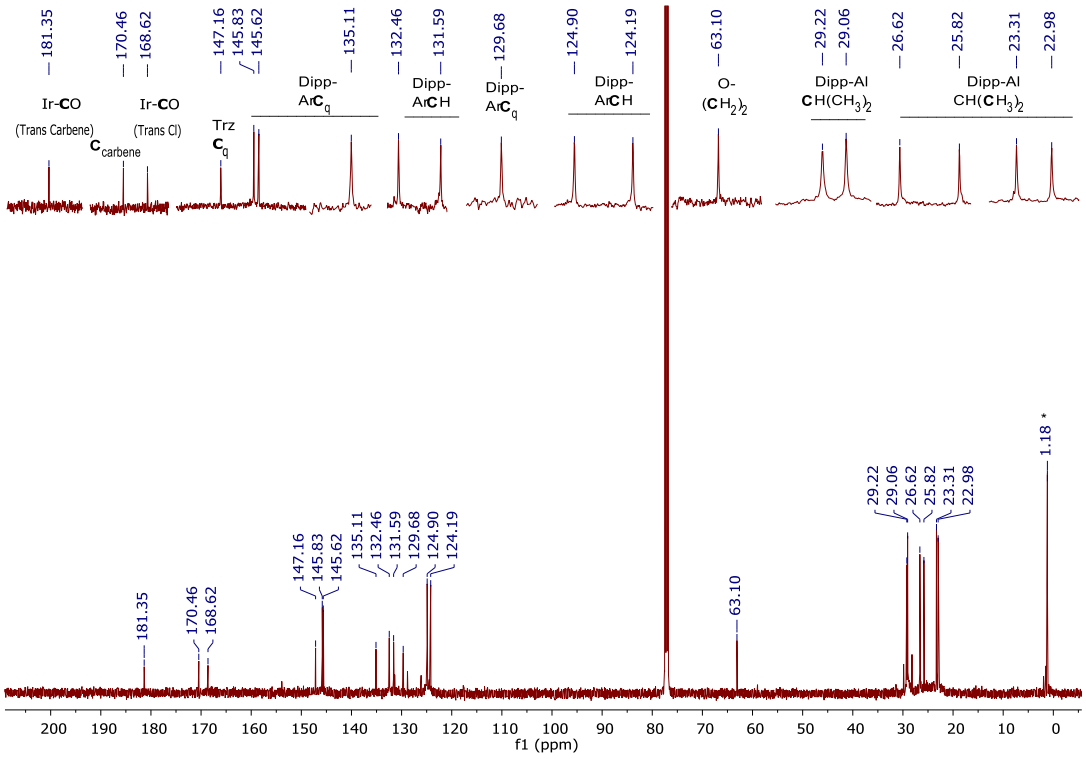

Figure S20: ^{13}C NMR spectrum of **4b** $[Ir_2(CO)_4Cl_2(\mu\text{-}\mathbf{COC})]$ in $CDCl_3$ [* annotates grease]

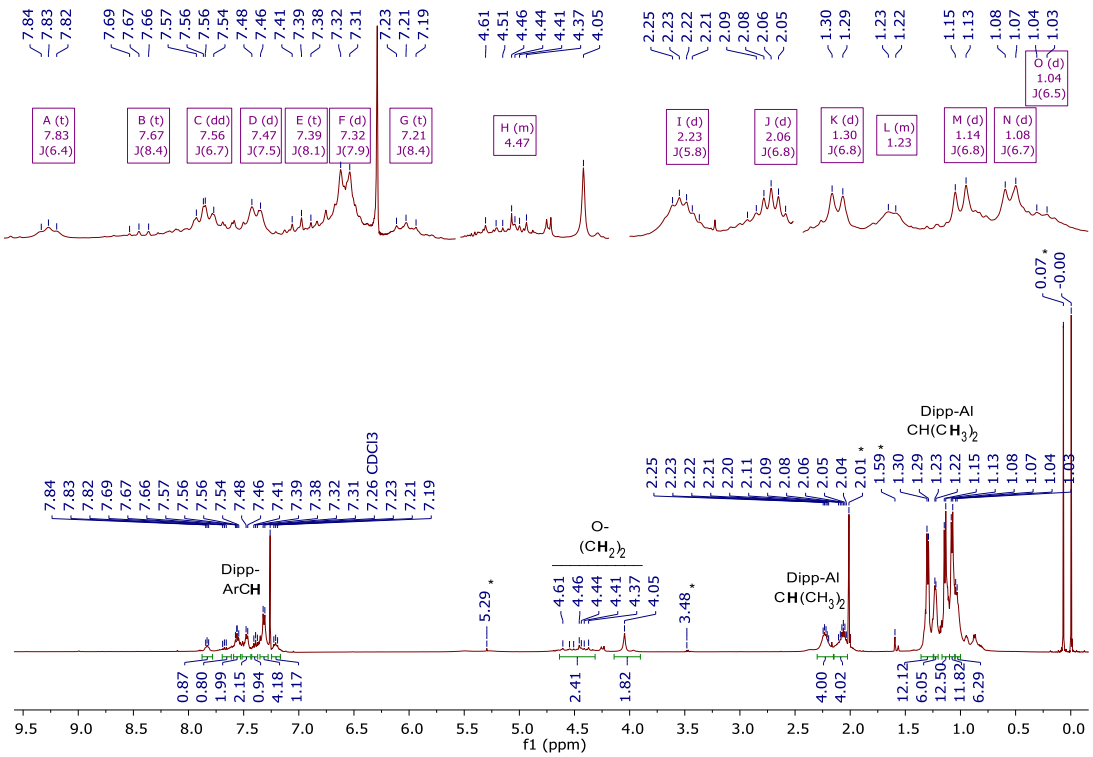

Figure S21: ^{1}H NMR spectrum of **5** [Ag_2Cl_2(μ-**COC**)] in $CDCl_3$

[* annotates residual DCM ($C\mathbf{H}_2$), diethyl ether ($C\mathbf{H}_2$) and grease]

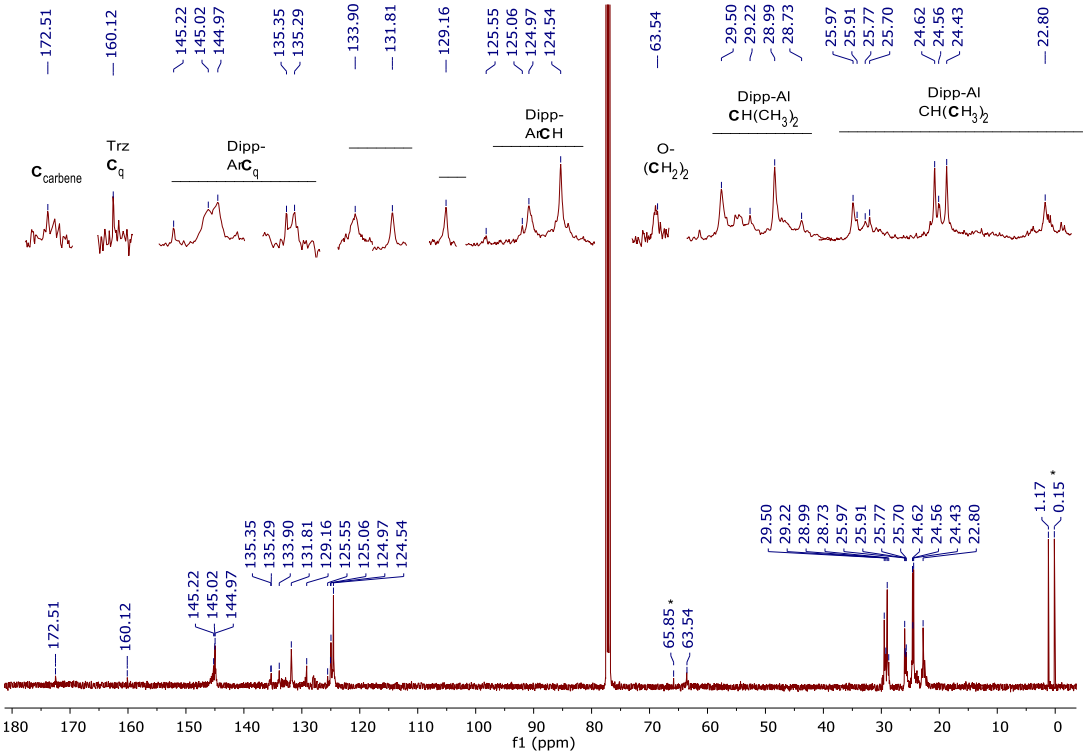

Figure S22: ^{13}C NMR spectrum of **5** [Ag_2Cl_2(μ-**COC**)] in $CDCl_3$

[* annotates residual diethyl ether ($C\mathbf{H}_2$) and grease]

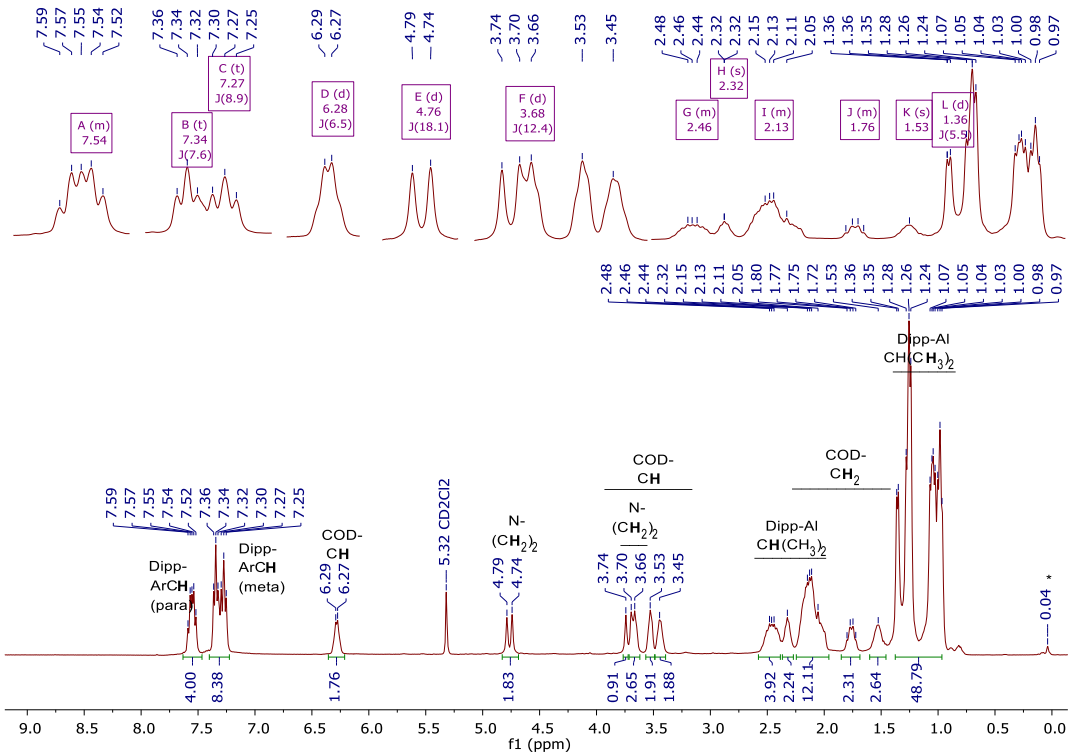

Figure S23: ^{1}H NMR spectrum (243 K) of **6** $[Rh_2(cod)_2(\mu\text{-}\mathbf{CNC})](PF_6)$ in CD_2Cl_2 [* annotates grease]

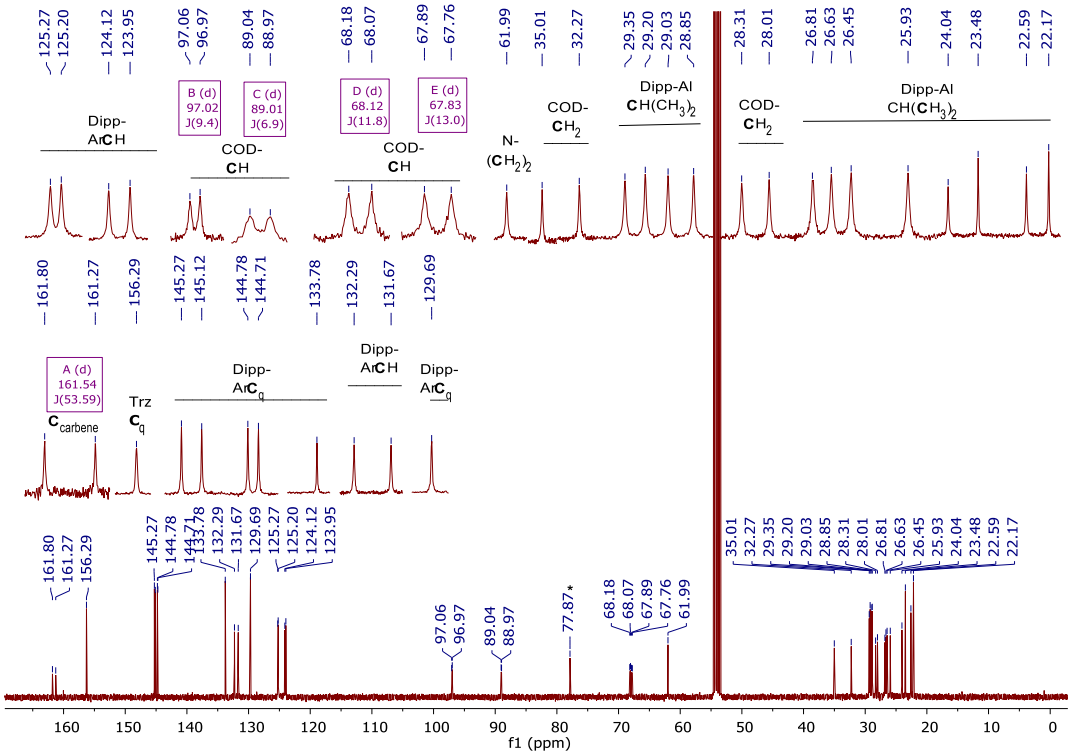

Figure S24: ^{13}C NMR spectrum (243 K) of **6** $[Rh_2(cod)_2(\mu\text{-}\mathbf{CNC})](PF_6)$ in CD_2Cl_2 [* annotates residual chloroform (**C**H)]

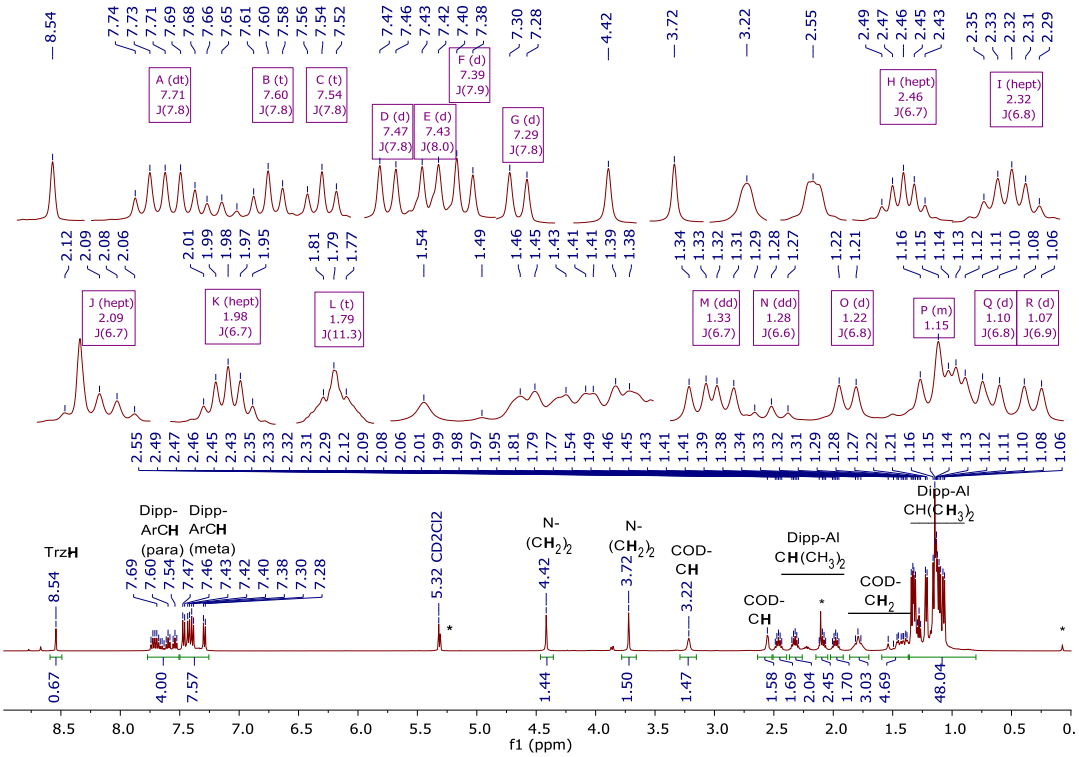

Figure S25: ^{1}H NMR spectrum of **7a** [Ir(cod)(**HCNC**)](PF$_6$) in CD_2Cl_2

[* annotates residual DCM (C**H**$_2$) and acetone (C**H**$_3$)]

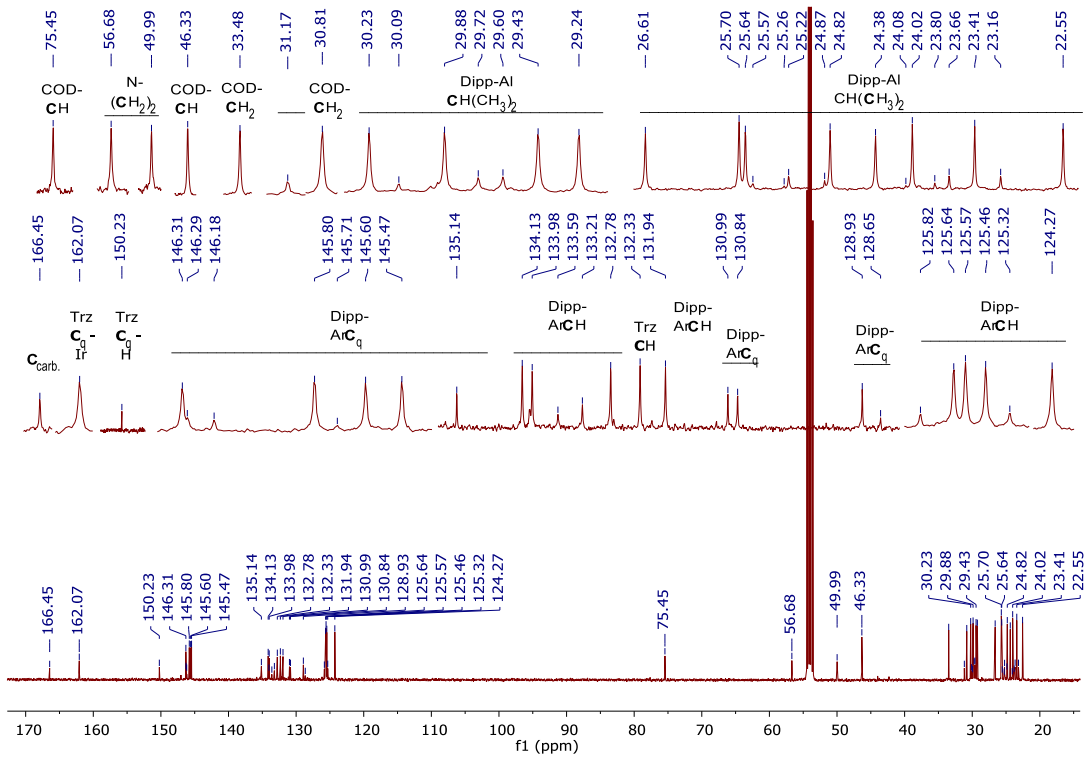

Figure S26: ^{13}C NMR spectrum of **7a** [Ir(cod)(**HCNC**)](PF$_6$) in CD_2Cl_2

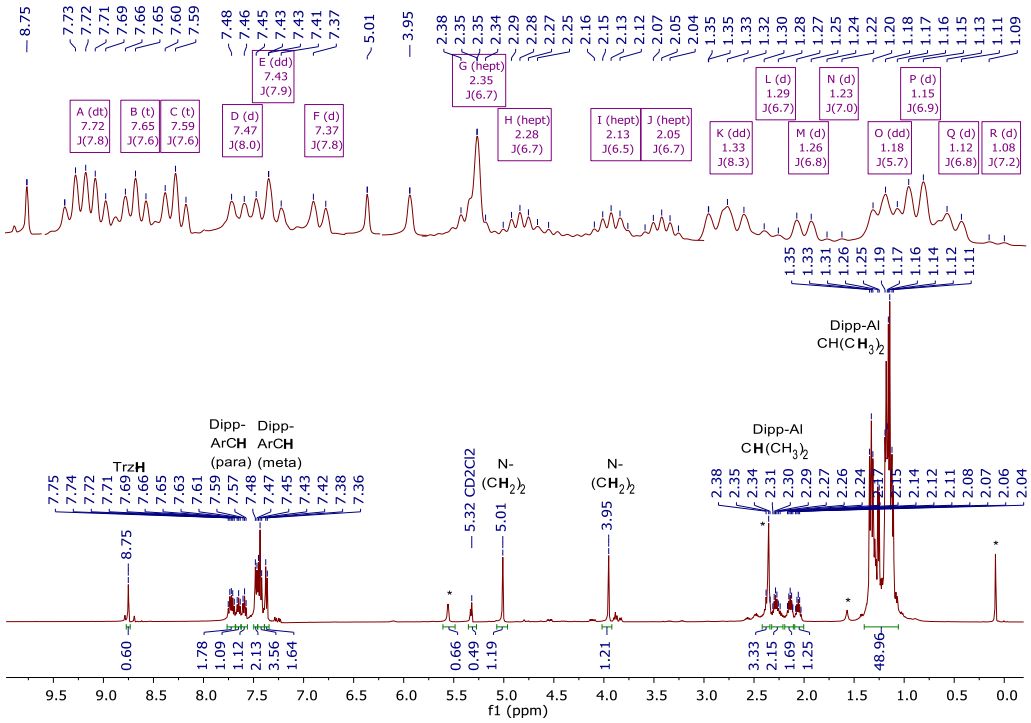

Figure S27: ^{1}H NMR spectrum of **7b** [Ir(CO)$_2$(**HCNC**)](PF$_6$) in CD_2Cl_2 [

* annotates free 1,5-cod, water (**H**$_2$O) and grease]

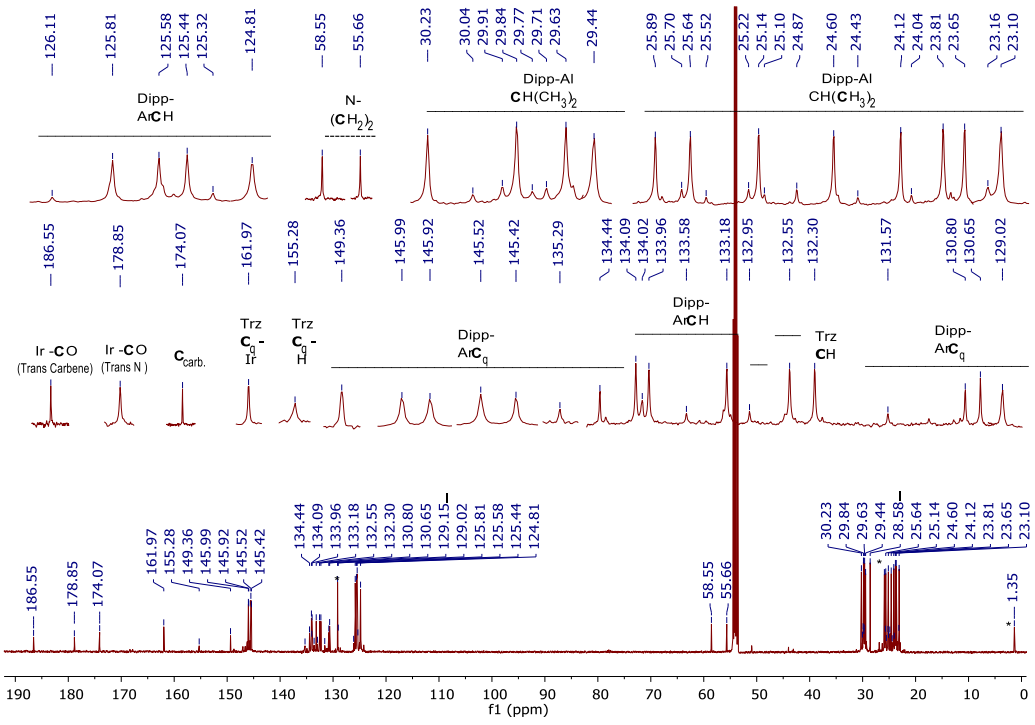

Figure S28: ^{13}C NMR spectrum of **7b** [Ir(CO)$_2$(**HCNC**)](PF$_6$) in CD_2Cl_2

[* annotates free 1,5-cod and grease]

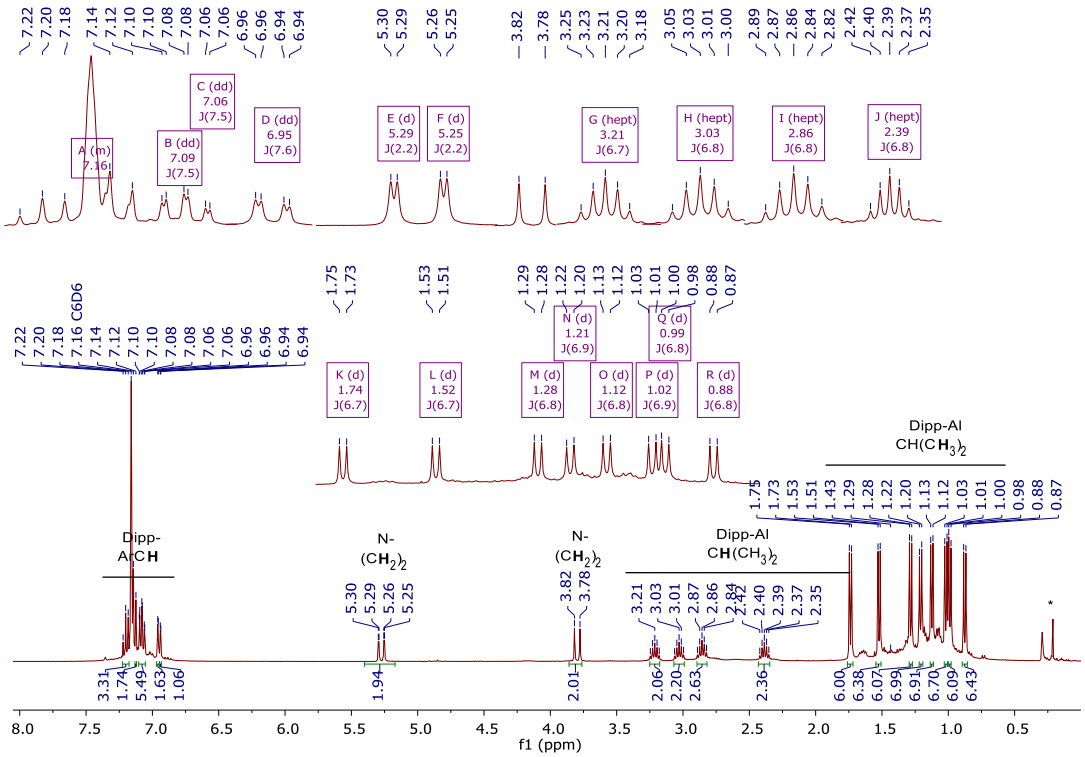

Figure S29: ^{1}H NMR spectrum of **8a** [$Rh_2(CO)_3Cl(\mu$-**CNC**)] in C_6D_6 [* annotates grease]

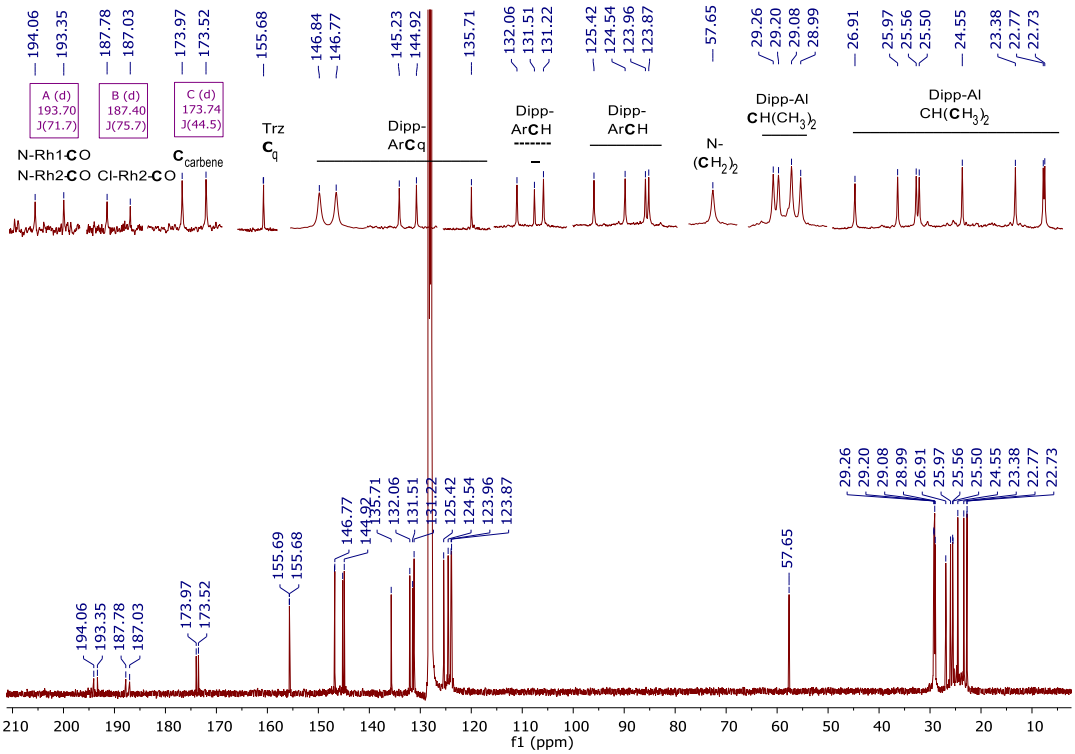

Figure S30: ^{13}C NMR spectrum of **8a** [$Rh_2(CO)_3Cl(\mu$-**CNC**)] in C_6D_6

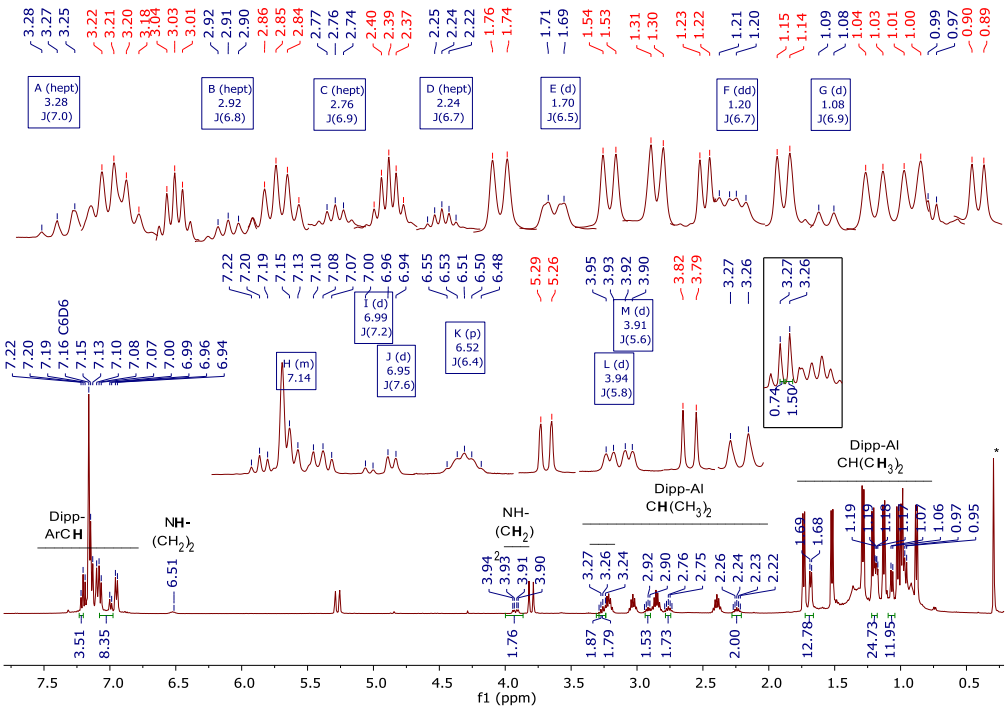

Figure S31: ^{1}H NMR spectrum of intractable mixture of **8a** $[Rh_2(CO)_3Cl(\mu\text{-}\mathbf{CNC})]$ (red) and **8b** $[Rh(CO)(\mathbf{C^HNC})](PF_6)$ (Blue) in C_6D_6 [* annotates grease]

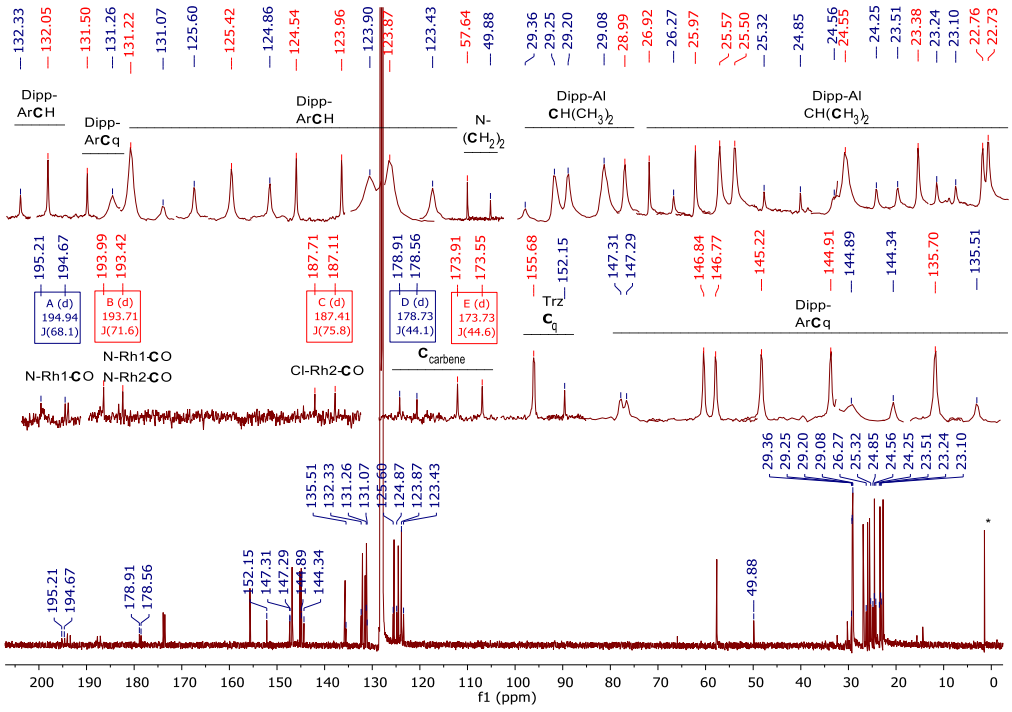

Figure S32: ^{13}C NMR spectrum of intractable mixture of **8a** $[Rh_2(CO)_3Cl(\mu\text{-}\mathbf{CNC})]$ (red) and **8b** $[Rh(CO)(\mathbf{C^HNC})](PF_6)$ (blue) in C_6D_6 [* annotates grease]

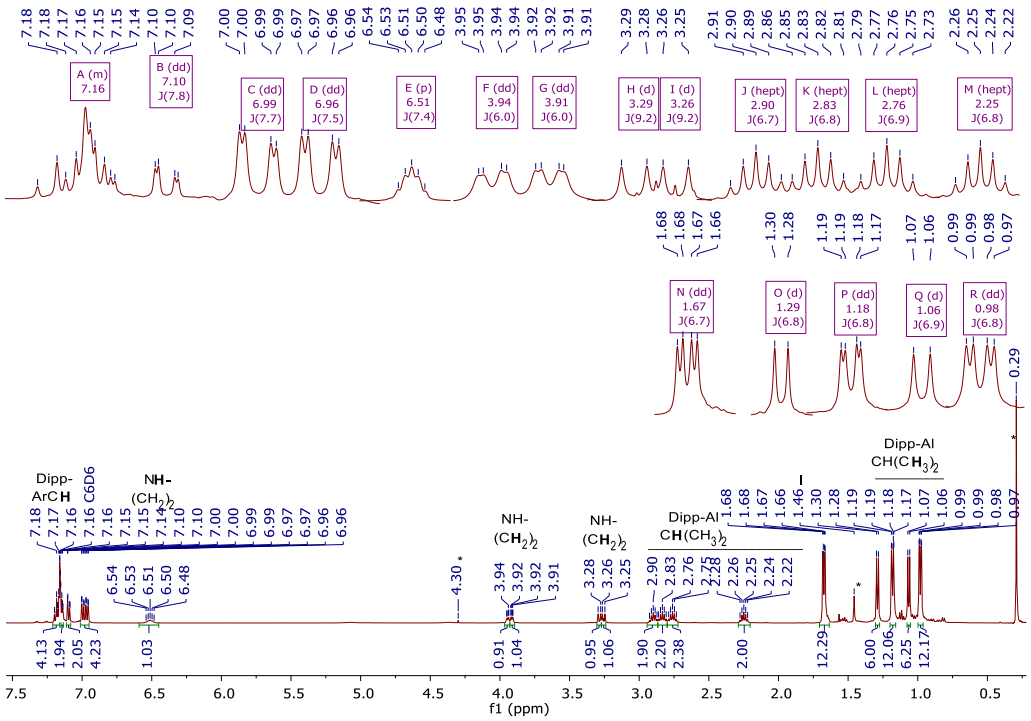

Figure S33: ^{1}H NMR spectrum of **8b** [Rh(CO)(C^{H}NC)](PF$_6$) in C_6D_6

[* annotates residual DCM (C**H**$_2$) and acetone (C**H**$_3$)]

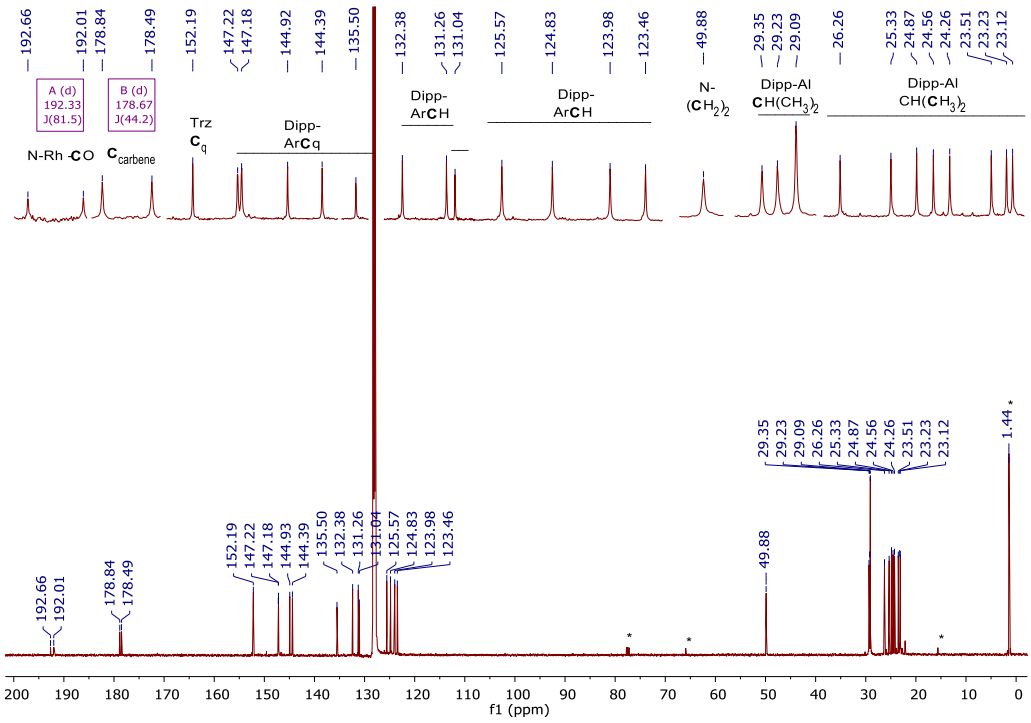

Figure S34: ^{13}C NMR spectrum of **8b** [Rh(CO)(C^{H}NC)](PF$_6$) in C_6D_6

[* annotates residual **C**DCl$_3$ & diethyl ether (**C**H$_2$ & **C**H$_3$)]

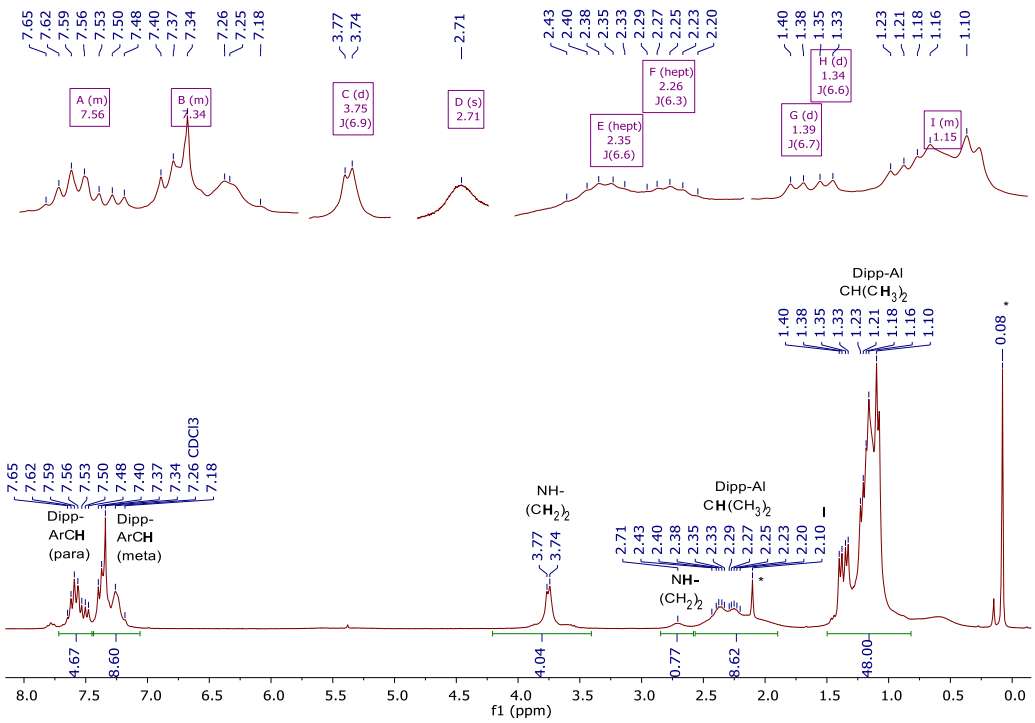

Figure S35: ^{1}H NMR spectrum of **9** [Ag_2Cl_2(μ-$C^{H}NC$)] in $CDCl_3$

[* annotates residual acetone (CH_3) and grease]

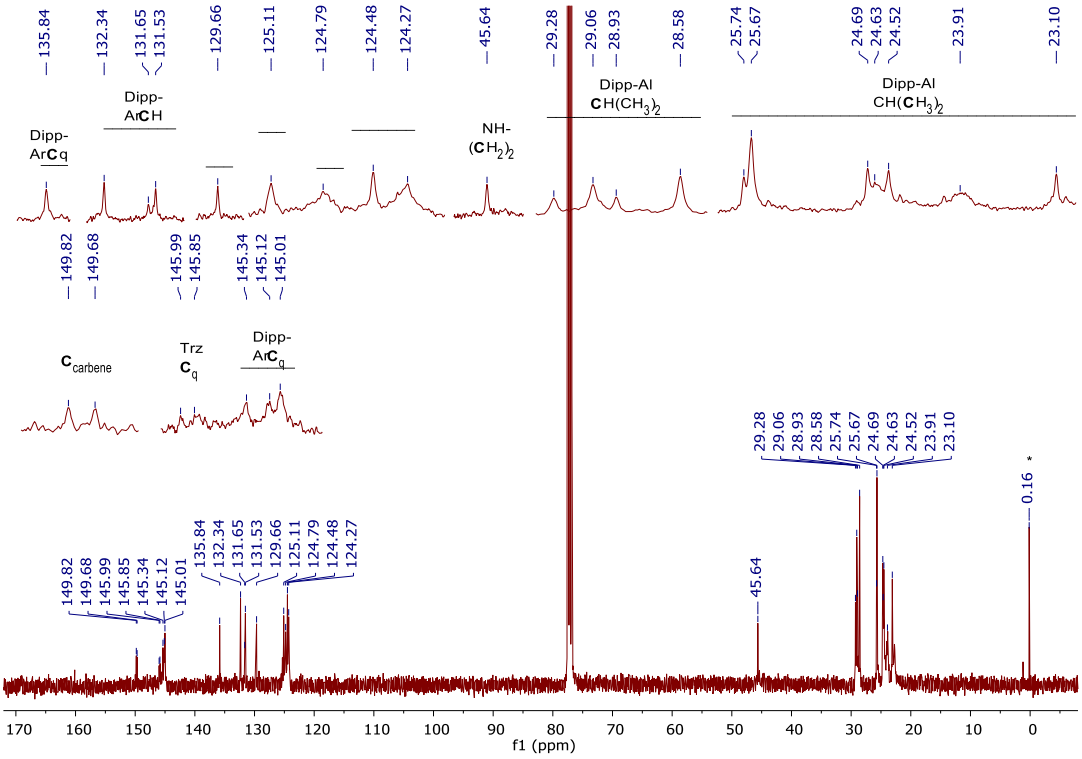

Figure S36: ^{13}C NMR spectrum of **9** [Ag_2Cl_2(μ-$C^{H}NC$)] in $CDCl_3$ [* annotates residual grease]

S4. Crystal Structure Details

Single crystal X-ray diffraction data were collected on Bruker D8 Venture kappa geometry diffractometers using Mo-K$_\alpha$ radiation (λ = 0.71073 Å) (*Iμs* for **1a** and sealed tube for **3a** and [H_2(**COC**)](PF_6)$_2$), Photon 100 CMOS detectors and *Apex3* control software.[7] A Bruker Apex II three circle diffractometer using sealed tube Mo-K$_\alpha$ radiation (λ = 0.71073 Å), CCD detector and *Apex2* control software [7] was used to collect data for [H_2(**C^{H}NC**)](PF_6)$_2$, [H_2(**C^{Boc}NC**)](PF_6)$_2$, **1b**, **2b**, **4a**, **6**, **7b** and **8a**. Crystals were selected under oil, mounted on nylon loops and then immediately placed in a cold stream of N_2 at 173 K or 150 K (for **1a**). Data reductions were performed using *SAINT,*[7] and multiscan absorption corrections were applied using *SADABS*[7] with the exception of **1b** where the raw data was used, and **1a** and **7a** where face-indexed absorption corrections using *XPREP*[7] were used. Structures were solved using *SHELXT-2018/2*[8] and refined using *SHELXL-2018/3*[9] and Olex2.[10] The crystal structures of [H_2(**COC**)](PF_6)$_2$, **3a**, **6**, **7b** and **8a** contained badly disordered solvent molecules. The contributions of these disordered molecules to the structure factors in these structures were calculated using *PLATON SQUEEZE*.[11]

S4.1 Crystal data for ligand salt [H_2(COC)](PF_6)$_2$

Suitable crystals of compound [H_2(**COC**)](PF_6)$_2$ for an X-ray diffraction analysis were obtained by slow solvent evaporation from DCM. $C_{54}H_{74}N_6OP_2F_{12}$ (M = 1113.13 g/mol): monoclinic, space group $P2_1/n$ (no.14), a = 12.3474(7) Å, b = 19.7123(10) Å, c = 13.7256(6) Å, α = 90°, β = 99.325(2)°, γ = 90°, V = 3296.6(3) Å^3, Z = 2, T = 173.15 K, μ(MoKα) = 0.137 mm^{-1}, *Dcalc* = 1.121 g/cm^3, 90921 reflections measured (5.836 ≤ Θ ≤ 50.996°), 5793 unique (6117 with I > 2σ(I)) (R_{int} = 0.0488, R_{sigma} = 0.0179) which were used in all calculations. The final R_1 was 0.0829 (I >2σ(I)) and wR_2 was 0.2246 (all data).

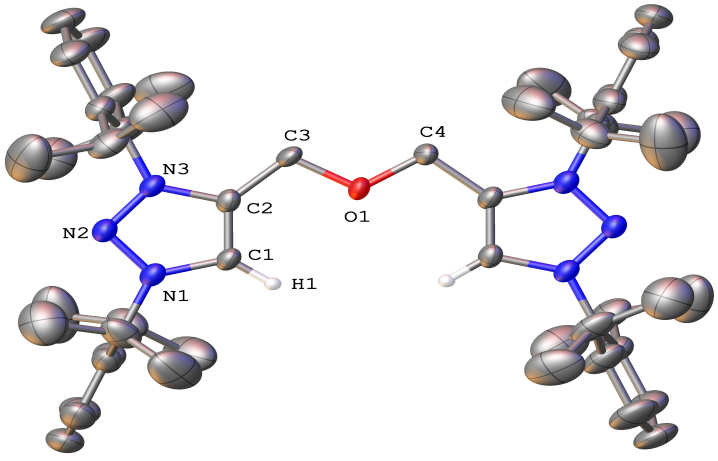

Figure S37. X-ray crystal structure of complex [H_2(**COC**)](PF_6)$_2$. (50% displacement ellipsoids)

[Counteranions ($2PF_6^-$) and hydrogen atoms (except for H1) omitted for clarity]

Selected bond distances (Å) and angles (º): C1-C2 1.366(4), C1-N1 1.351(4), C2-N3 1.352(4), C2-C3 1.475(6), N2-N3 1.325(3), N2-N1 1.326(3), C3-O1 1.414(4), C4-O1 1.401(7), N1-C1-C2 105.6(2), C1-C2-C3 134.7(3), C2-C3-01 103.3(4), C3-O1-C4 113.2(4), C1-N1-N2 112.7(2), N1-N2-N3 103.6(2), N2-N3-C2 113.0(2), N3-C2-C3 120.1(3).

S4.2 Crystal data for ligand salt $[H_2(C^{Boc}NC)](PF_6)_2$

Suitable crystals of compound $[H_2(\mathbf{C^{Boc}NC})](PF_6)_2$ for an X-ray diffraction analysis were obtained by slow solvent evaporation from DCM. $C_{59}H_{85}N_7O_3P_2F_{12}$ (Incl. solvent H_2O) (M = 1230.27 g/mol): monoclinic, space group $P2_1/n$ (no.14), a = 19.8012(13) Å, b = 12.6035(9) Å, c = 26.5305(19) Å, α = 90°, β = 105.6995(18)°, γ = 90°, V = 6374.1(8) Å^3, Z = 4, T = 173.15 K, μ(MoKα) = 0.151 mm^{-1}, *Dcalc* = 1.282 g/cm^3, 72816 reflections measured (5.614 ≤ Θ ≤ 51.456°), 12121 unique (6117 with I > 2σ(I)) (R_{int} = 0.0482, R_{sigma} = 0.0395) which were used in all calculations. The final R_1 was 0.0619 (I >2σ(I)) and wR_2 was 0.1552 (all data).

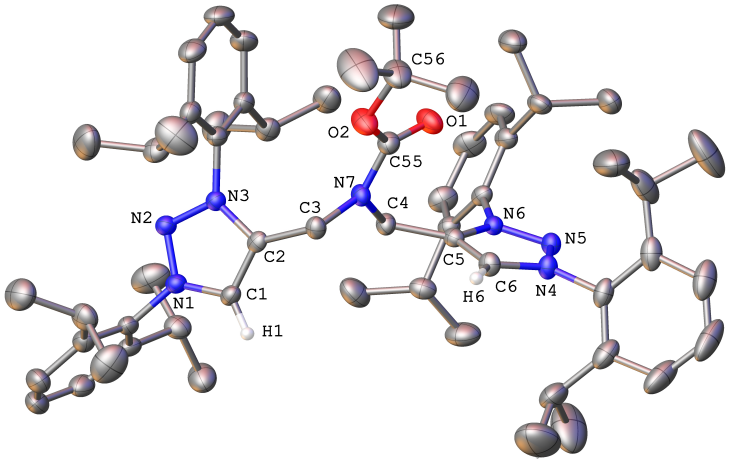

Figure S38. X-ray crystal structure of complex $[H_2(\mathbf{C^{Boc}NC})](PF_6)_2$. (50% displacement ellipsoids) [Counteranions ($2PF_6^-$), hydrogen atoms (except for H1 and H6) and solvent molecules (H_2O) omitted for clarity]

Selected bond distances (Å) and angles (º): C1-C2 1.358(3), C1-N1 1.352(3), C2-C3 1.493(3), C2-N3 1.364(3), C3-N7 1.460(3), C4-C5 1.491(3), C4-N7 1.454(3), C5-C6 1.361(3), C5-N6 1.363(3), C6-N4 1.354(3), C55-N7 1.366(3), C55-O1 1.207(3), C55-O2 1.332(3), C56-O2 1.482(3), N1-N2 1.327(3), N2-

N3 1.328(3), N4-N5 1.325(3), N5-N6 1.326(3); C1-C2-C3 129.9(2), C2-C3-N7 112.97(19), C3-N7-C4 118.63(19), C4-C5-C6 132.9(2), C3-N7-C55 124.41(19).

S4.3 Crystal data for ligand salt $[H_2(C^{H}NC)](PF_6)_2$

Suitable crystals of compound $[H_2(C^{H}NC)](PF_6)_2$ for an X-ray diffraction analysis were obtained by slow solvent evaporation from DCM / CH_3CN mixture. $C_{56}H_{78}N_8P_2F_{12}$ (incl. CH_3CN) (M = 1153.20 g/mol): triclinic, space group P-1 (no.2), a = 11.0352(2) Å, b = 12.3798(2) Å, c = 24.3690(4) Å, α = 81.3850(10)°, β = 89.281(10)°, γ = 65.5350(10)°, V = 2991.51(9) Å^3, Z = 2, T = 173.15 K, μ(MoKα) = 0.153 mm^{-1}, *Dcalc* = 1.280 g/cm^3, 122057 reflections measured (3.386 ≤ Θ ≤ 56.71°), 14937 unique (6117 with I > 2σ(I)) (R_{int} = 0.0415, R_{sigma} = 0.0280) which were used in all calculations. The final R_1 was 0.0443 (I >2σ(I)) and wR_2 was 0.1226 (all data).

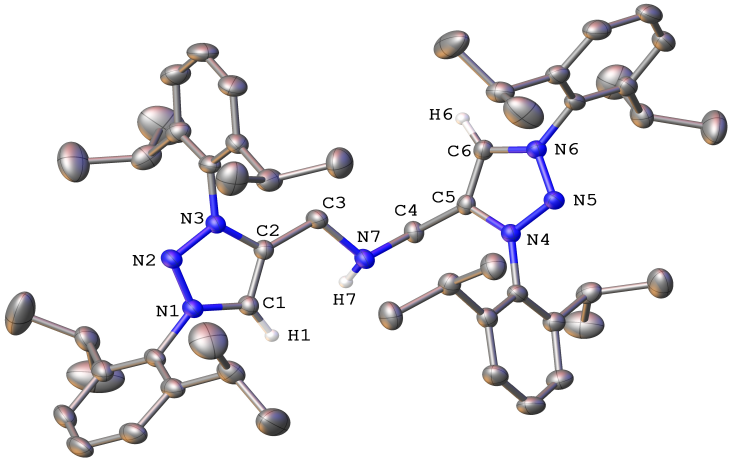

Figure S39. X-ray crystal structure of complex $[H_2(C^{Boc}NC)](PF_6)_2$. (50% displacement ellipsoids) [Counteranions ($2PF_6^-$), hydrogen atoms (except for H1, H6 and H7) and solvent molecules (CH_3CN) omitted for clarity] Selected bond distances (Å) and angles (º): C1-C2 1.3670(17), C1-N1 1.3518(16), C2-C3 1.4901(18), C2-N3 1.3606(16), C3-N7 1.4553(17), C4-C5 1.4987(17), C4-N7 1.4652(16), C5-C6 1.3636(18), C5-N4 1.3688(16), C6-N6 1.3521(16), N1-N2 1.3258(14), N2-N3 1.3280(15), N4-N5 1.3264(14), N5-N6 1.3240(14), C1-C2-C3 132.14(12), C2-C3-N7 109.64(10), C3-N7-C4 112.46(10), C4-C5-C6 131.50(12).

S4.4 Crystal data for complex 1b [Ir(cod)(COC)](PF$_6$).

Suitable crystals of compound **1b** [Ir(cod)(**COC**)](PF_6) for an X-ray diffraction analysis were obtained by slow solvent evaporation from a toluene / DCM mixture. $C_{65}H_{90}N_6OCl_6IrPF_6$ (Incl. 6 DCM) (M = 1521.29

g/mol): triclinic, space group *P* -1 (no.2), *a* = 15.0178(9) Å, *b* = 15.1067(9) Å, *c* = 18.2934(10) Å, α = 76.729(3)°, *β* = 69.064(3)°, γ = 65.711(3)°, *V* = 3516.4(4) Å^3, *Z* = 2, *T* = 173.15 K, μ(MoKα) = 2.209 mm^{-1}, *Dcalc* = 1.437 g/cm^3, 144803 reflections measured (2.972 ≤ Θ ≤ 57.152°), 17852 unique (6117 with I > 2σ(I)) (R_{int} = 0.0358, R_{sigma} = 0.0226) which were used in all calculations. The final R_1 was 0.0264 (I >2σ(I)) and wR_2 was 0.0687 (all data).

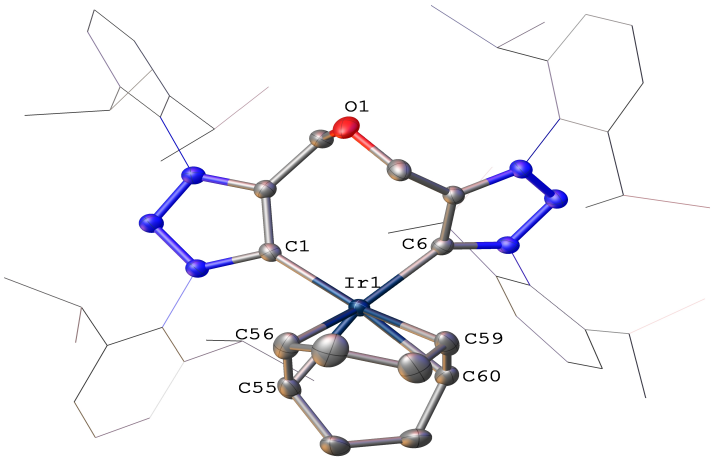

Figure S40. X-ray crystal structure of complex **1b** [Ir(cod)(**COC**)](PF$_6$). (50% displacement ellipsoids) [Counteranion (PF$_6^-$), hydrogen atoms and solvent molecules (DCM) omitted for clarity]

Selected bond distances (Å) and angles (º): Ir1-C1 2.102(2), Ir1-C6 2.055(2), Ir1-C55 2.223(2), Ir1-C56 2.162(2), Ir1-C59 2.177(2), Ir1-C60 2.152(2), C1–Ir1–C6 92.74(8), C1–Ir1–C55 98.27(8), C1–Ir1–C56 91.90(9), C1–Ir1–C59 159.12(10), C1–Ir1–C60 163.36(10), C6–Ir1–C55 168.04(9), C6–Ir1–C56 147.91(10), C6–Ir1–C59 84.29(9), C6–Ir1–C60 89.29(9).

S4.5 Crystal data for complex 2a [Rh(CO)$_2$(COC)](PF$_6$).

Suitable crystals of compound **2a** [Rh(CO)$_2$(**COC**)](PF$_6$) for an X-ray diffraction analysis were obtained by slow solvent evaporation from DCM. $C_{56}H_{72}N_6O_3RhPF_6$ (*M* =1125.07 g/mol): monoclinic, space group *Pc* (no. 7), *a* = 21.5202(11) Å, *b* = 10.7072(5) Å, *c* = 24.8940(13) Å, *β* = 105.722(2)°, *V* = 5521.5(5) Å^3, *Z* = 4, *T* = 150.0 K, μ(MoKα) = 0.407 mm^{-1}, *Dcalc* = 1.353 g/cm^3, 209908 reflections measured (4.364° ≤ 2Θ ≤ 53.554°), 23488 unique (R_{int} = 0.0588, R_{sigma} = 0.0365) which were used in all calculations. The final R_1 was 0.0313 (I > 2σ(I)) and wR_2 was 0.0643 (all data).

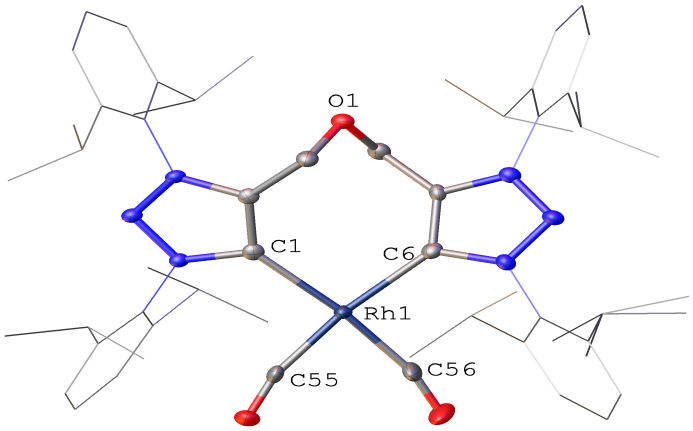

Figure S41. X-ray crystal structure of complex **2a** $[Rh(CO)_2(\mathbf{COC})](PF_6)$. (50% displacement ellipsoids) [Counteranion (PF_6^-) and hydrogen atoms omitted for clarity]

Selected bond distances (Å) and angles (º): Rh1-C1 2.122(4), Rh1-C6 2.110(4), Rh1-C55 1.878(4), Rh1-C56 1.878(4), C1–Rh1–C6 95.24(14), C1–Rh1–C55 93.09(15), C1–Rh1–C56 167.67(17), C6–Rh1–C55 167.76(15), C6–Rh1–C56 90.90(16).

S4.6 Crystal data for complex 2b $[Ir(CO)_2(COC)](PF_6)$

Suitable crystals of compound **2b** $[Ir(CO)_2(\mathbf{COC})](PF_6)$ for an X-ray diffraction analysis were obtained by slow solvent evaporation from C_6D_6. $C_{56}H_{72}N_6O_3IrPF_6$ (M =1214.36 g/mol): monoclinic, space group $P2_1/c$ (no.14), a = 21.527(3) Å, b = 10.6934(14) Å, c = 24.942(3) Å, α = 90°, β = 105.386(9)°, V = 5535.7(13) Å^3, Z = 4, T = 150.15 K, μ(MoKα) = 2.509 mm^{-1}, *Dcalc* = 1.457 g/cm^3, 72636 reflections measured (3.388° ≤ 2Θ ≤ 50°), 9747 unique (R_{int} = 0.5670, R_{sigma} = 0.5490) which were used in all calculations. The final R_1 was 0.0895 (I > 2σ(I)) and wR_2 was 0.1964 (all data).

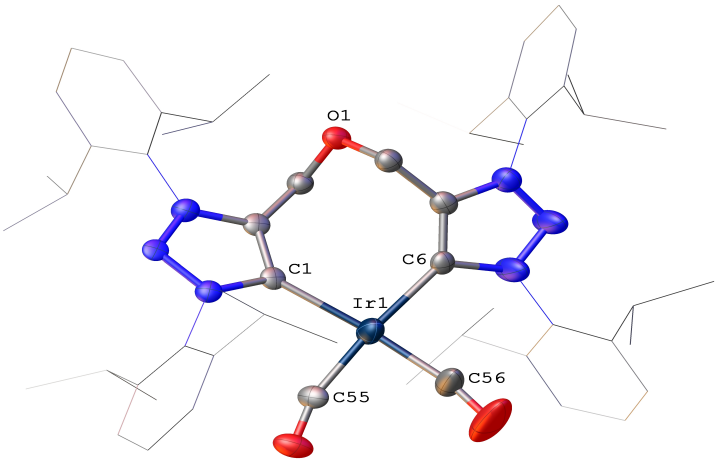

Figure S42. X-ray crystal structure of complex **2b** $[Ir(CO)_2(\mathbf{COC})](PF_6)$. (50% displacement ellipsoids) [Counteranion (PF_6^-) and hydrogen atoms omitted for clarity]

Selected bond distances (Å) and angles (º): Ir1-C1 2.110(16), Ir1-C6 2.059(15), Ir1-C55 1.824(17), Ir1-C56 1.868(19), C1–Ir1–C6 93.7(6), C1–Ir1–C55 91.5(7), C1–Ir1–C56 169.2(8), C6–Ir1–C55 172.6(7), C6–Ir1–C56 92.7(7).

S4.7 Crystal data for complex 3a $[Rh_2(cod)_2Cl_2(\mu\text{-}COC)]$

Suitable crystals of compound **3a** $[Rh_2(cod)_2Cl_2(\mathbf{\mu\text{-}COC})]$ for an X-ray diffraction analysis were obtained by slow solvent evaporation from $CDCl_3$. $C_{71}H_{98}Cl_4N_6ORh_2$ (M =1399.17 g/mol): monoclinic, space group $P2_1/c$ (no. 14), a = 15.4130(8) Å, b = 35.913(2) Å, c = 15.0642(8) Å, β = 111.6130(10)°, V = 7752.2(7) Å^3, Z = 4, T = 173.15 K, μ(MoKα) = 0.605 mm^{-1}, *Dcalc* = 1.199 g/cm^3, 113394 reflections measured (5.686° ≤ 2Θ ≤ 55.996°), 18698 unique (R_{int} = 0.0458, R_{sigma} = 0.0264) which were used in all calculations. The final R_1 was 0.0411 (I > 2σ(I)) and wR_2 was 0.0968 (all data).

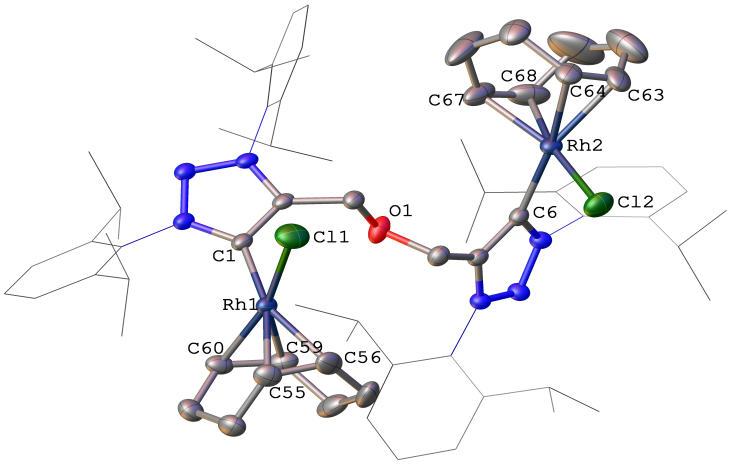

Figure S43. X-ray crystal structure of complex **3a** $[Rh_2(cod)_2Cl_2(\mathbf{\mu\text{-}COC})]$. (50% displacement ellipsoids) (Hydrogen atoms and solvent molecules (DCM) omitted for clarity)

Selected bond distances (Å) and angles (º): Rh1-C1 2.030(2), Rh1-Cl1 2.3927(7), Rh1-C55 2.197(3), Rh1-C56 2.177(3), Rh1-C59 2.099(3), Rh1-C60 2.089(2), Rh2-C6 2.043(2), Rh2-Cl2 2.3741(7), Rh2-C63 2.167(3), Rh2-C64 2.205(2), Rh2-C67 2.087(3), C1–Rh1–Cl1 86.46(7), C55–Rh1–C1 165.77(10), C56–Rh1–C1 157.78(10), C59–Rh1–C1 94.40(10), C60–Rh1–C1 93.06(9), C6–Rh2–Cl2 87.31(7), C6–Rh2–C63 155.92(11), C6–Rh2–C64 167.10(10), C6–Rh2–C67 95.81(10), C6–Rh2–C68 93.60(11)

S4.8 Crystal data for complex 4a [$Rh_2(CO)_4Cl_2(\mu$-COC)]

Suitable crystals of compound **4a** [$Rh_2(CO)_4Cl_2(\mu$-**COC**)] for an X-ray diffraction analysis were obtained by slow solvent evaporation from $CDCl_3$. $C_{58}H_{72}N_6O_5Cl_2Rh_2$ (M = 1209.93 g/mol): triclinic, space group P -1 (no. 2), a = 10.4449(4) Å, b = 15.9061(6) Å, c = 17.7631(7) Å, α = 87.305(2)°, β = 76.657(2)°, γ = 88.372(2)°, V = 2867.81(19) Å^3, Z = 2, T = 173.15 K, μ(MoKα) = 0.720 mm^{-1}, *Dcalc* = 1.401 g/cm^3, 35559 reflections measured (2.564 ≤ Θ ≤ 51.564°), 10990 unique (6117 with I > 2σ(I)) (R_{int} = 0.0844, R_{sigma} = 0.1074) which were used in all calculations. The final R_1 was 0.0568 (I >2σ(I)) and wR_2 was 0.1402 (all data).

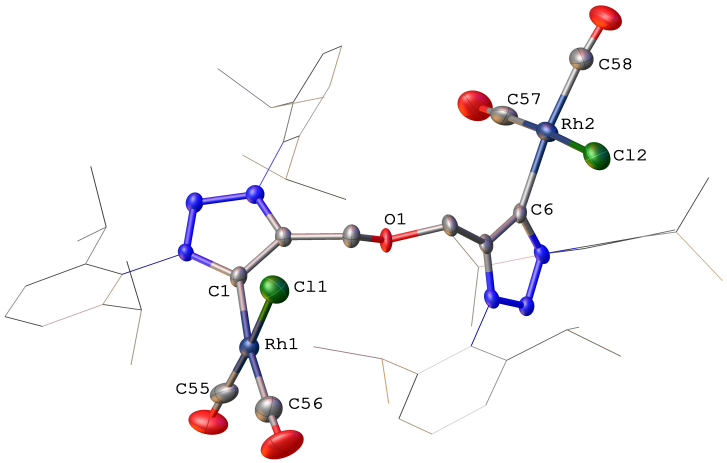

Figure S44. X-ray crystal structure of complex **4a** [$Rh_2(CO)_4Cl_2(\mu$-**COC**)]. (50% displacement ellipsoids) (Hydrogen atoms omitted for clarity)

Selected bond distances (Å) and angles (º): Rh1-C1 2.054(5), Rh1-Cl1 2.3434(16), Rh1-C55 1.831(7), Rh1-C56 1.899(7), Rh2-C6 2.041(5), Rh2-Cl2 2.3672(17), Rh2-C57 1.812(7), Rh2-C58 1.905(6), C1–Rh1–Cl1 87.50(15), C55–Rh1–C1 93.1(2), C56–Rh1–C1 172.9(2), C6–Rh2–Cl2 85.70(15), C6–Rh2–C57 91.6(2), C6–Rh2–C58 174.0(2).

S4.9 Crystal data for complex 6 [$Rh_2(cod)_2(\mu$-CNC)](PF_6)

Suitable crystals of compound **6** [$Rh_2(cod)_2(\mu$-**CNC**)](PF_6) for an X-ray diffraction analysis were obtained by slow solvent evaporation from a toluene / DCM mixture. $C_{73}H_{102}N_7Cl_6Rh_2PF_6$ (Incl. 3 DCM) (M = 1641.10 g/mol): triclinic, space group P -1 (no.2), a = 12.4173(11) Å, b = 16.7357(16) Å, c = 20.3867(18) Å, α = 81.880(6)°, β = 85.642(6)°, γ = 86.607(6)°, V = 4177.0(7) Å^3, Z = 2, T = 173.15 K, μ(MoKα) = 0.661 mm^{-1}, *Dcalc* = 1.302 g/cm^3, 59766 reflections measured (2.022 ≤ Θ ≤ 50°), 14704

unique (6117 with I > 2σ(I)) (R_{int} = 0.0858, R_{sigma} = 0.0824) which were used in all calculations. The final R_1 was 0.1040 (I >2σ(I)) and wR_2 was 0.2779 (all data).

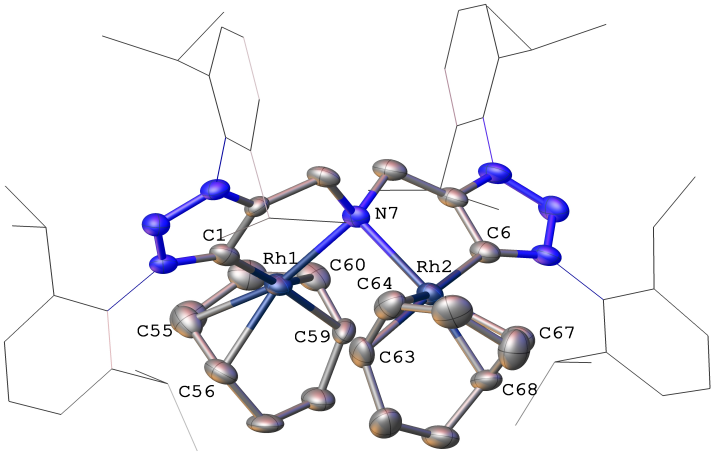

Figure S45. X-ray crystal structure of complex **6** $[Rh_2(cod)_2(\mu\text{-}\mathbf{CNC})](PF_6)$. (50% displacement ellipsoids) [Counteranion (PF_6^-), hydrogen atoms and solvent molecules (DCM) omitted for clarity]

Selected bond distances (Å) and angles (º):Rh1-Rh2 3.1963(12), Rh1-C1 2.035(11), Rh2-C6 2.037(10), Rh1-N7 2.209(8), Rh2-N7 2.217(8), Rh1-C55 2.125(12), Rh1-C56 2.136(11), Rh1-C59 2.223(11), Rh1-C60 2.191(11), Rh2-C63 2.207(11), Rh2-C64 2.179(12), Rh1–N7– Rh2 92.5(3), C1–Rh1–N7 80.8(4), C1–Rh1–C55 93.9(4), C1–Rh1–C56 94.7(4), C1–Rh1–C59 169.6(4), C1–Rh1–C60 153.9(4), C6–Rh2–C63 167.9(4), C6–Rh2–C64 156.4(4), C6–Rh2–C67 95.4(5), C6–Rh2–C68 95.3(4).

S4.10 Crystal data for complex 7b $[Ir(CO)_2(HCNC)](PF_6)$

Suitable crystals of compound **7b** $[Ir(CO)_2(H\mathbf{CNC})](PF_6)$ for an X-ray diffraction analysis were obtained from DCM / Hexane by slow vapour diffusion. $C_{58}H_{77}Cl_4F_6IrN_7O_2P$ (Incl. 2 DCM) (M =1383.23 g/mol): triclinic, space group P-1 (no. 2), a = 12.0336(7) Å, b = 13.6319(9) Å, c = 22.5444(15) Å, α = 96.465(5)°, β = 104.140(4)°, γ = 97.574(4)°, V = 3514.3(4) Å^3, Z = 2, T = 173.15 K, μ(MoKα) = 2.131 mm^{-1}, *Dcalc* = 1.307 g/cm^3, 34784 reflections measured (3.048° ≤ 2Θ ≤ 50°), 12322 unique (R_{int} = 0.1339, R_{sigma} = 0.1557) which were used in all calculations. The final R_1 was 0.0770 (I > 2σ(I)) and wR_2 was 0.1845 (all data).

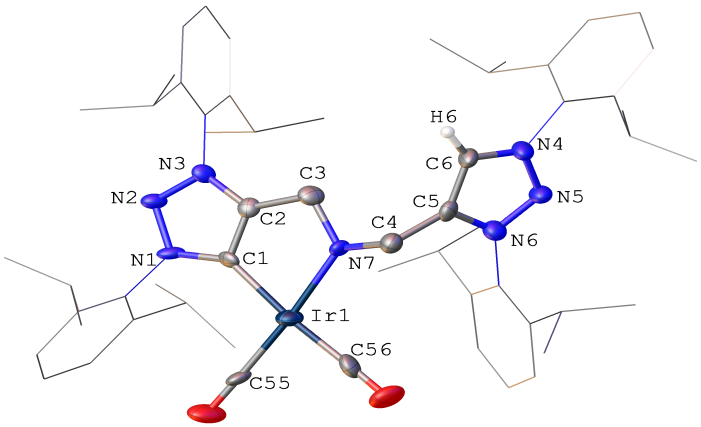

Figure S46. X-ray crystal structure of complex **7b** [Ir(CO)$_2$(H**C**N**C**)](PF$_6$). (50% displacement ellipsoids) (Hydrogen atoms, counteranion (PF_6^-) and solvent molecules (DCM) omitted for clarity)

Selected bond distances (Å) and angles (º): Ir1-C1 2.032(9), Ir1-N7 2.048(7), Ir1-C55 1.865(9), Ir1-C56 1.866(11), C1–Ir1–N7 78.0(3), C1–Ir1–C55 97.2(3), C1–Ir1–C56 174.3(4), N7–Ir1–C55 175.3(3), N7–Ir1–C56 96.3(3).

S4.10 Crystal data for complex 8a [Rh$_2$(CO)$_3$Cl(μ-CNC)]

Suitable crystals of compound **8a** [Rh$_2$(CO)$_3$Cl(μ-**C**N**C**)] for an X-ray diffraction analysis were obtained by slow solvent evaporation from toluene. $C_{57}H_{72}N_7O_3ClRh_2$ (M = 1144.48 g/mol): triclinic, space group *P* -1 (no.2), *a* = 10.7323(18) Å, *b* = 13.222(2) Å, *c* = 21.491(3) Å, *α*= 82.115(3)°, *β* = 78.984(4)°, *γ* = 86.235(3)°, *V* = 2962.7(8) Å^3, *Z* = 2, *T* = 173.15 K, μ(MoKα) = 0.648 mm^{-1}, *Dcalc* = 1.283 g/cm^3, 18554 reflections measured (3.112 ≤ Θ ≤ 51°), 10960 unique (6117 with I > 2σ(I)) (R_{int} = 0.0869, R_{sigma} = 0.1565) which were used in all calculations. The final R_1 was 0.0758 (I >2σ(I)) and wR_2 was 0.2273 (all data).

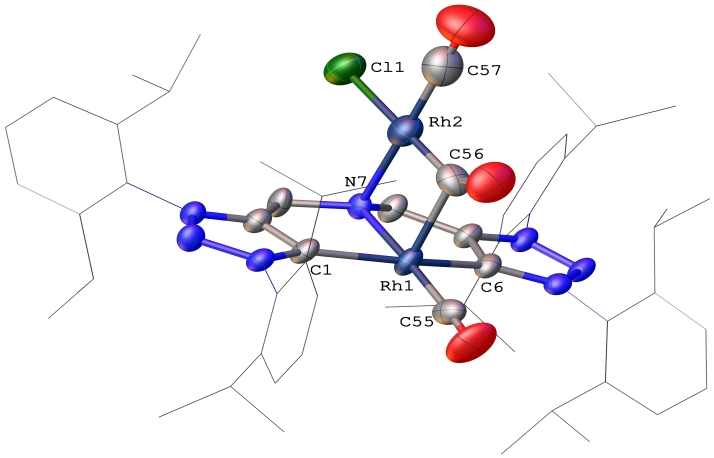

Figure S47. X-ray crystal structure of complex **8a** [$Rh_2(CO)_3Cl(\mu$-**CNC**)]. (50% displacement ellipsoids) (Hydrogen atoms omitted for clarity)

Selected bond distances (Å) and angles (º): Rh1-Rh2 2.9698(12), Rh1-C1 2.046(8), Rh1-C6 2.029(8), Rh1-N7 2.113(6), Rh1-C55 1.846(10), Rh1-C56 2.211(10), Rh2-N7 2.189(7), Rh2-C56 1.909(11), Rh2-C57 1.819(15), Rh2-Cl1 2.385(3), C1–Rh1–C6 157.3(3), C1–Rh1–N7 79.3(3), C1–Rh1–C55 100.0(3), N7–Rh1–C56 87.3(3), Rh1–N7–Rh2 56 47.41(18), N7–Rh2–C57 177.7(4).

S5. References

1) (a) Nimitsiriwat, N.; Gibson, V. C.; Marshall, E. L.; Takolpuckdee, P.; Tomov, A.K.; White, A. J. P.; Williams, D. J.; Elsegood, M. R. J.; Dale, S. H. Mono- versus bis-chelate formation in triazenide and amidinate complexes of magnesium and zinc. *Inorg. Chem*. **2007**, *46*, 9988-9997. (b) Barrett, A. G. M.; Crimmin, M. R.; Hill, M. S.; Hitchcock, P. B.; Kociok-Kohn, G.; Procopiou, P. A. Triazenide complexes of the heavier alkaline earths: Synthesis, characterization, and suitability for hydroamination catalysis. *Inorg Chem*. **2008**, *47*, 7366-7376.

2) (a) Mintz, C.; Walling, M. J. t-Butyl Hypochlorite. *Org. Synth*. **1969**, *49*, 9. (b) Wirschun, W.; Winkler, M.; Lutz, K.; Jochims, J. C. 1,3-Diaza-2-azoniaallene salts: Cycloadditions to alkynes, carbodiimides and cyanamides. *J.Chem.Soc., Perkin Trans. 1,* **1998**, *0*, 1755-1762.

3) Wu, J.; Lu, W.-Y.; Hou, J.-L.; Li, C.; Wu, Z.-Q.; Jiang, X.-K.; Li, Z.-T.; Yu, Y.-H.; Dynamic [2]Catenanes Based on a Hydrogen Bonding-Mediated Bis-Zinc Porphyrin Foldamer Tweezer: A Case Study. *J. Org. Chem*. **2007**, *72*, 2897-2905.

4) Giordano G.; and Crabtree, R. H. Inorganic Syntheses: Reagents for Transition metal complex and Organometallic Syntheses, J. Wiley & Sons, Hoboken. **1991**, *28*, 88.

5) McCleverty, J. A.; Wilkinson, G. Inorganic Syntheses: Reagents for Transition metal complex and Organometallic Syntheses, J. Wiley & Sons, Hoboken. **1991**, *28*, 84.

6) a) Inorganic Syntheses: Reagents for Transition metal complex and Organometallic Syntheses, J. Wiley & Sons, Hoboken. **1974**, *15*, 19. b) Choudhury, J.; Poddler, S.; Roy, S, Cooperative Friedel−Crafts Catalysis in Heterobimetallic Regime: Alkylation of Aromatics by π-Activated Alcohols. *J. Am. Chem. Soc.*, **2005**, *127* (17), 6162–6163.

7) Bruker (2012). Apex2, Apex3, Saint, SADABS, XPREP. Bruker AXS Inc., Madison, Wisconsin, USA.

8) Sheldrick, G. M. *SHELXT* – Integrated space-group and crystal-structure determination. (2015). *Acta Cryst.*, **2015**, *A71*, 3-8.

9) Sheldrick, G. M. Crystal structure refinement with SHELXL. *Acta Cryst.,* **2015**, *C71*, 3-8.

10) Dolomanov, O. V.; Bourhis, L. J.; Gildea, R. J.; Howard, J. A. K.; Puschmann, H. Olex2: A complete structure solution, refinement and analysis program. *J. Appl. Cryst.* **2009**, *42*, 339-341.

11) Spek, A. L. *PLATON* Squeeze: a tool for the calculation of the disordered solvent contribution to the calculated structure factors. *Acta Cryst.,* **2015**, *C71*, 9-18.